Pharmacological Characterization of Drug Candidates Targeting Receptors

January 2023

Ryokichi KOYAMA

Pharmacological Characterization of Drug Candidates Targeting Receptors

A Dissertation Submitted to

the Graduate School of Science and Technology,

University of Tsukuba

in Partial Fulfillment of Requirements

for the Degree of Doctor of Philosophy in Science

Doctoral Program in Biology,

Degree Programs in Life and Earth Sciences

Ryokichi KOYAMA

Table of Contents

Abstract

In this research, I focused on molecular mechanisms of receptors, especially Retinoic acid-related orphan receptor gamma t (RORγt) and G protein-coupled receptor 40 (FFAR1/GPR40). RORγt is a member of the nuclear receptor (NR), and the expression of the receptor is limited to several immune cell types, such as Th17 cells. Th17 cells produce IL-17 and play an important role in cell host immunity against fungi and bacteria, while induce tissue inflammation linked with autoimmune diseases. This IL-17 expression is transcriptionally induced by RORγt, therefore RORγt inverse agonist would be potential for autoimmune diseases. GPR40 is a GPCR expressed in pancreatic islet and enteroendocrine cells, and its agonism is known to improve glycemic control in diabetes. Fasiglifam (TAK-875, Phase 3 terminated), a first-generation GPR40 partial agonist, effectively controls hyperglycemia in patients with type 2 diabetes. Compared with fasiglifam, an advanced full agonist for GPR40 is more effective in controlling glucose levels in rodent models compared to partial agonists.

In this study, I conducted molecular biological analysis for these receptors and their selective modulators. In addition, GPR40 agonism was evaluated *in vivo* assay. First, I analyzed inhibition mechanism of known RORγt inverse agonist, TO901317, using recombinant RORγt proteins. As a result, I revealed that cholesterol within the Ligand Binding Pocket (LBP) of the recombinant RORγt protein hampers the potency of RORγt inverse agonist. By utilizing apo-protein, I successfully identified Compound 1 as a novel cholesterol competitive RORγt inverse agonist. Second, I analyzed molecular mechanism of SCO-267, a novel GPR40 full agonist by using GPR40 overexpressed stable cell lines. Consequently, I revealed that SCO-267 allosterically activates Gαq, Gαs, Gα12/13 signaling, and β-arrestin recruitment. I also confirmed SCO-267's durability in cell lines and diabetic rat model. These results provide new evidence of molecular mechanism of both RORγt and GPR40 modulators, and also would be impactful and applicable to drug development against other NHRs and GPCRs.

Abbreviations

AC: Adenylate cyclase

AF-1: Activator Function-1 region

AF-2: Activator Function-2 region

AR: Androgen receptor

AP-2: Adaptor protein complex-2

BSA: Bovine serum albumin

cAMP: Cyclic AMP

CCL18: Chemokine ligand 18

CCL21: Chemokine ligand 21

CCR7: C-C chemokine receptor type 7

CI: Confidence interval

DAG: Diacylglycerol

DBD: DNA binding domain

DC_{50}: Half-maximal desensitization concentration

DHA: Docosahexaenoic Acid

DPBS: Dulbecco's phosphate-buffered saline

DTT: Dithiothreitol

E. coli: *Escherichia coli*

ER: Estrogen receptor

FBS: Fetal bovine serum

FRET: Fluorescence Resonance Energy transfer

GDP: Guanosine diphosphate

GLP-1: Glucagon-like peptide 1

GPR40: G protein-coupled receptor 40 / Free fatty acid receptor 1 / FFAR1

GPR120: G protein coupled receptor 120 / Free fatty acid receptor 4 / FFAR4

GR: Glucocorticoid receptor

GRK: G protein-coupled receptor kinase

GEF: Guanine-nucleotide exchange factor

GTP: Guanosine triphosphate

GRK: G protein-coupled receptor kinase

G418: Geneticin

HbA1c: Hemoglobin A1c

HNF4: Hepatocyte nuclear factor 4

hRORγt (*E. coli*): Human RORγt protein expressed in *E. coli*

hRORγt (Ins): Human RORγt protein expressed in insect cells

HTRF: Homogeneous time-resolved fluorescence
HTS: High-throughput screening
IL-17: Interleukin-17
IPTG: Isopropyl β-D-1-thiogalactopyranoside
IP1: Myo-inositol 1 phosphate
ITT: Insulin tolerance test
LBD: Ligand binding domain
LBP: ligand binding pocket
LXR: Liver X receptor
MAPK: Mitogen-activated protein kinase
MEM-α: Minimum essential medium-α
NAFLD: Nonalcoholic fatty liver disease
NK cell: Natural Killer cell
NR: Nuclear receptor
N-STZ rat: Neonatally streptozotocin-induced diabetic rat
NTD: N-terminal domain
OGTT: Oral glucose tolerance test
PK: Protein kinase
PTHR: parathyroid hormone receptor type 1 receptor
RORγt: Retinoic acid-related orphan receptor gamma t
RORα: Retinoic acid-related orphan receptor alpha
RORβ: Retinoic acid-related orphan receptor beta
RORγ: Retinoic acid-related orphan receptor gamma
ROREs: ROR response elements
RXR: Retinoid X receptor
Sf-9: Spodoptera frugiperda Sf9 cells
SRF-RE: Serum response factor response element
STZ: streptozotocin
TCEP: Tris(2-carboxyethyl) phosphine
TEV: Tobacco Etch Virus
TSA: Thermal shift assay
T2DM: type 2 diabetes mellitus
PKA: Protein kinase A
PKC: Protein kinase C
PLCβ: Phospholipase C beta
PPAR: Peroxisome proliferator-activated receptor

TR: Thyroid hormone receptor

VDR: Vitamin D receptor

V2R: V2 Vasopressin receptor

General Introduction

Receptors

In multicellular organism, a well-organized network of communication between cells was necessary for smooth control of the entire organism. By evoking biological response through receiving signals, cells adapt their behavior to the condition of the environment. This maintenance of an optimal physiological environment is known as homeostasis. One of the key players of the homeostasis are receptors. The receptors recognize environmental stimuli, then pass the information to intracellular molecules leading to change of cell metabolism and gene regulation, which is signal transduction. Receptors are localized at cellular membrane or intracellularly (Fig. 1). One important family of intracellular receptors are the nuclear receptors located in the cytoplasm or even inside the nucleus. Cellular membrane receptors are classified into several groups based on the structure. Ligand gated ion channels are pore-forming membrane proteins that allow target ions to pass through the pore in response to ligand binding. GPCRs are also known as 7-Transmembrane receptors containing seven hydrophobic transmembrane segments. Receptor tyrosine kinases have a kinase domain which phosphorylates the receptor itself with dimerization by ligand binding. Interaction between adaptor proteins and the phosphorylated receptor leads to the initiation of signal transduction pathways. Overington *et al*. reported that targets of almost 50% of drugs were GPCRs, NRs, and ligand gated ion channels based on the gene-family distribution analysis of drug substance [1]. This result suggests that these receptors are regarded as attractive drug target families.

Molecular Pharmacology of Receptors

As shown in Fig. 2, a molecule or chemical compound that can bind and activate a receptor to elicit a biological response is named as “Agonist”. Among them, “Full agonist” activates the receptor fully, in contrast “Partial agonist” does not retain the ability to functionally activate the receptor fully. On the other hand, “Antagonist” binds to a receptor and inhibits the biological response by an agonist. “Inverse agonist” binds to a receptor and inactivates the constitutive activity in the absence of an agonist. In contrast, these molecules are also classified as to binding sites [2]. An orthosteric site is the binding site for the endogenous agonist, while an allosteric site is the binding site distinct from the orthosteric site (Fig. 3). Allosteric modulator can bind to the receptor at the same time as an orthosteric ligand, which is ternary complex, and cause a change in affinity or efficacy of the ligand. Binding of an allosteric modulator increases the affinity of a receptor for orthosteric ligand, which is called positive cooperativity, while the decrease in the affinity is negative cooperativity. Allosteric modulators have three advantages compared with orthosteric molecules [2]. First, the effect of allosteric modulators is saturable, which means that once the allosteric sites are occupied, no additional allosteric effect is observed. Second, they can

be only selectively effective in tissues in which the endogenous ligand works physiologically. Third advantage is the potential for greater receptor selectivity because generally allosteric sites are unique for a particular protein, in contrast with orthosteric sites common to a set of protein such as ATP or hormone agonist [3].

Nuclear Receptors

NR superfamily is composed of a family of transcription factors that play several roles in various physiological response including metabolism, reproduction, cell proliferation, and inflammation [4, 5]. Since the first member of this family, GR, was cloned in 1985, now the NR family consists of 48 members [6].

Although the biological process by NR is vast, these proteins share a common modular domain structure [7] (Fig. 4). The NTD (A/B region) is non-conserved and a highly disordered domain. The NTD contains AF-1 domain, which interacts with various co-regulator proteins in a cell-specific style [8]. The DBD (C region) is the most conserved domain, which is responsible for the interaction between NRs and specific DNA sequences. LBD (E region) not only binds to specific ligands but also interacts directly with various co-regulator proteins through conformational change by ligand binding. The LBD contains AF-2 domain and the C-terminal helix12. Without ligand, corepressors interact with the AF-2 surface resulted in suppression of gene transcription. Ligand binding cause conformational changes with repositioning helix12, which allows for recognition of coactivators [9]. Recruitment of coactivators initiates the protein complex formation including histone modifying enzymes, general transcriptional machinery, and RNA Polymerase II to drive gene-specific transcription [10] (Fig. 5).

Orphan NR

In the1980s and 1990s, function of ER, AR, GR, TR and VDR were clarified by using known and natural ligands [11]. These NRs have structural similarities and conserved domains of these NRs. With the advanced molecular techniques and the generation of the cDNA library from various tissues, new NRs were identified [12]. These new receptors have a lack of endogenous ligand information, so named “orphan NRs”. As orphan NRs was discovered, research focused on the identification of potential ligands using receptors for screening. This method allowed for the screening of not only ligand but also natural or synthetic compounds regulating the receptors. Once a ligand or a compound for target orphan NR has been identified, these tools are helpful for understanding the receptor’s physiological functions, resulted in the development of novel therapeutic strategy. For example, identification of 9-cis-retinoic acid as RXR endogenous ligand resulted in the discovery of RXR heterodimerization with numerous other NRs as a mechanism of controlling gene-specific expression [13]. PPARs are the first orphan NRs found to form

heterodimerization with RXR, and PPARγ, one of the PPAR subtypes, is a target of thiazolidinedione class of drugs which are used for treatment of type 2 diabetes through increasing insulin sensitivity [14]. Thus, identification of a ligand or a small compound for orphan NRs is important because activation or inactivation of the receptor by these molecules could expand our knowledge about the receptor's biological function and involvement of disease progression.

GPCRs

GPCRs are large class of plasma membrane proteins and play important roles of biological process such as neurological, cardiovascular, endocrine, and reproductive functions [15, 16]. Their endogenous ligands include hormones, neurotransmitters, chemokines, lipids, and peptides. Among 826 human GPCRs, approximately 350 members are regarded as druggable and 527 drugs targeting GPCRs are already approved by United States Food and Drug Administration [17]. Thus, GPCRs are a major target in drug discovery and an area of biological research interest. Upon ligand binding, GPCRs undergo conformational change inducing GDP to GTP exchange in Gα proteins and dissociation of Gαβγ complexes (Fig. 6). Then, activated GTP-bound Gα protein activates/inhibits downstream effector proteins depending on the Gα subunit type including Gαs, Gαi, Gαq, and Gα12/13 [18]. Gαs activates AC, resulted in the conversion of ATP into cAMP which activates PKA leading to downstream response. In contrast, Gαi inhibits AC with a decrease in intracellular cAMP levels [19]. Gαq activates PLCβ, in turn, cleaves PIP2 into IP3 and DAG. IP3 stimulates the secretion of Ca^{2+} into the cytosol, while DAG activates PKC localized at plasma membrane. Gα12/13 activates small monomeric GTPase Rho A, in turn, modulates various downstream effector systems [20]. GPCRs phosphorylated by GRK interact with β-arrestin mediating receptor internalization as well as G-protein-independent signaling [21].

GPCR trafficking

One of the GPCR regulation mechanisms is their endocytic trafficking. In order to prevent excessive stimulation in cells and maintain a homeostasis, GPCRs stimulated by ligands tend to undergo cyclical process of receptor activation, desensitization, and resensitization (Fig. 7). Agonist binding leads to G-protein dependent signaling followed by phosphorylation of GPCRs by PK and β-arrestin recruitment. The GPCR-β-arrestin complex interacts with AP-2 and clathrin for endocytosis. Dynamin is required for membrane fission during endocytosis. Once internalized, some receptors exhibit signal transduction. Then, the receptors are trafficked to recycling endosomes or targeted to lysosomes for degradation. Receptors which are recycled back to the plasma membrane can be activated as resensitized receptors [22, 23]. These post-endocytic fates and desensitization rates are thought to be dependent on GPCRs and agonist compounds, so understanding the trafficking of a target GPCR is important for drug development of a chronic

disease.

In this thesis, I focused on the molecular biological mechanisms of receptors, especially RORγt, one of orphan NRs, and GPR40, one of GPCRs. In the first chapter, to elucidate the relationship on the RORγt protein between an inverse agonist and an endogenous ligand, I examined the effect of cholesterol against the RORγt inverse agonists' activity by *in vitro* experiments. Furthermore, identification of a novel RORγt inverse agonist through HTS is also described. In the second chapter, to clarify the molecular mechanism and sustained action of GPR40 stimulated by a GPR40 full agonist, I conducted signaling analysis using GPR40 overexpressed cells and a long-term experiment using diabetic rat model. The results of these studies provide an insight into molecular mechanisms of these receptors with new chemical tool compounds, and drug discovery against the other NHRs and GPCRs.

Figures

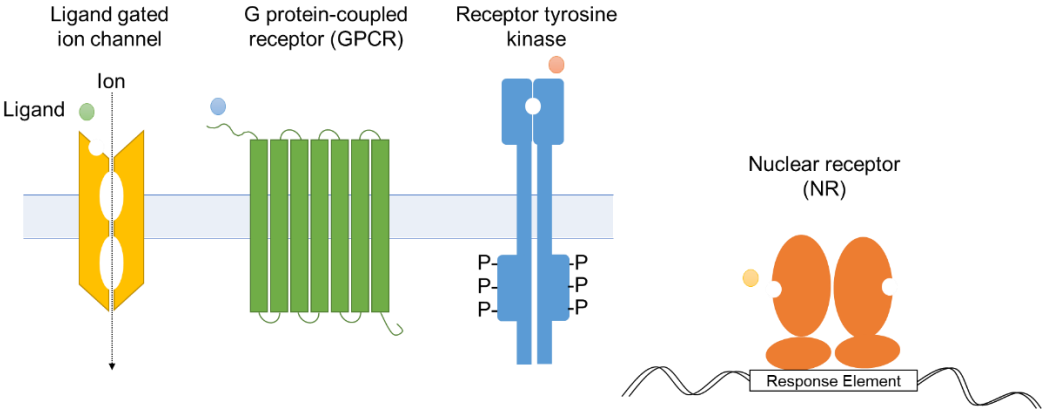

Figures 1. Schematic representation of receptor structures

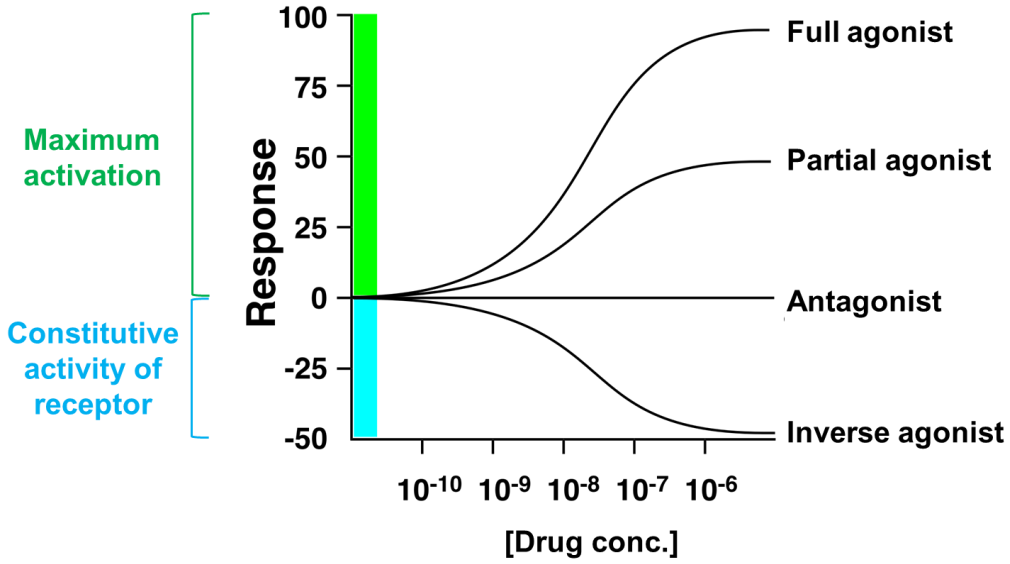

Figure 2. Schematic representation of receptor pharmacology

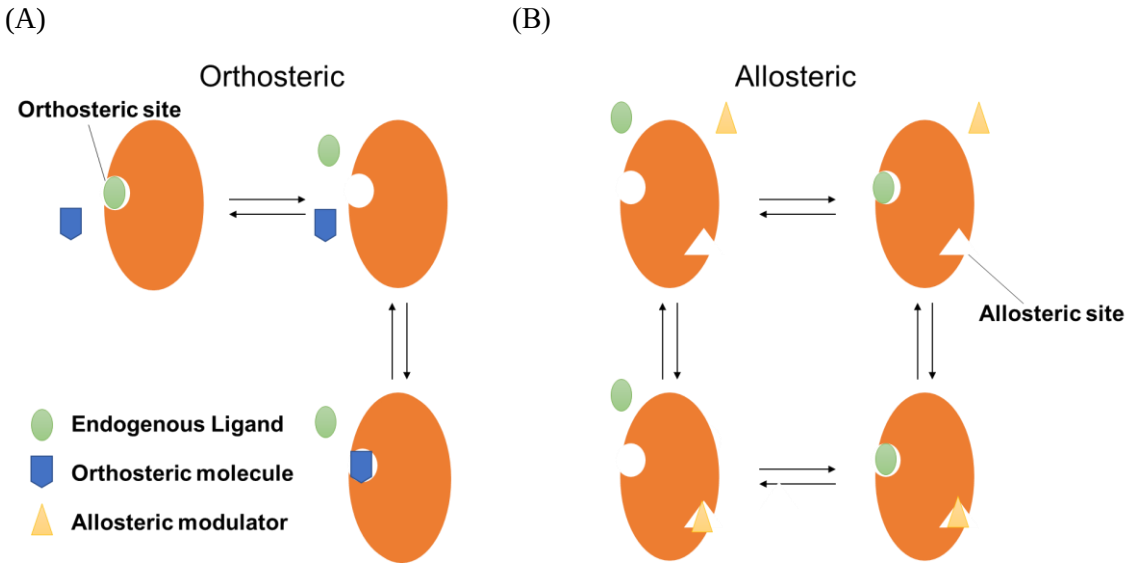

Figure 3. Schema of orthosteric binding (A) and allosteric binding (B)

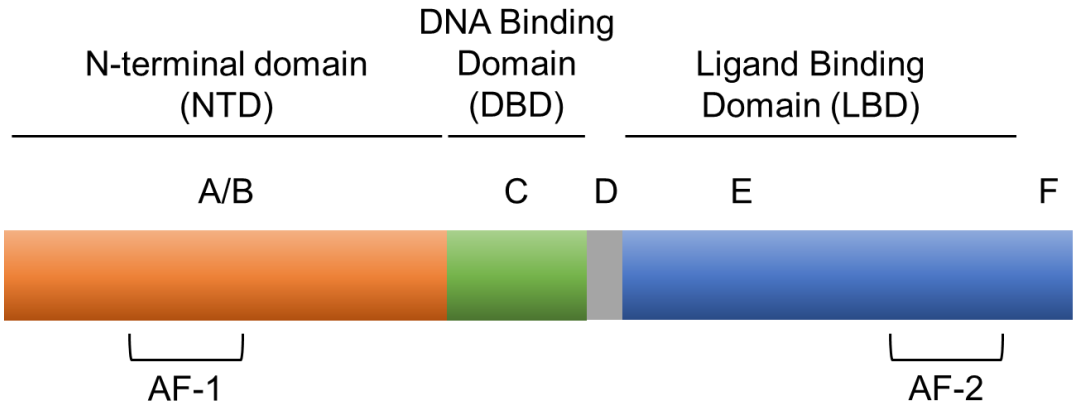

Figure 4. Schematic representation of structure of NRs

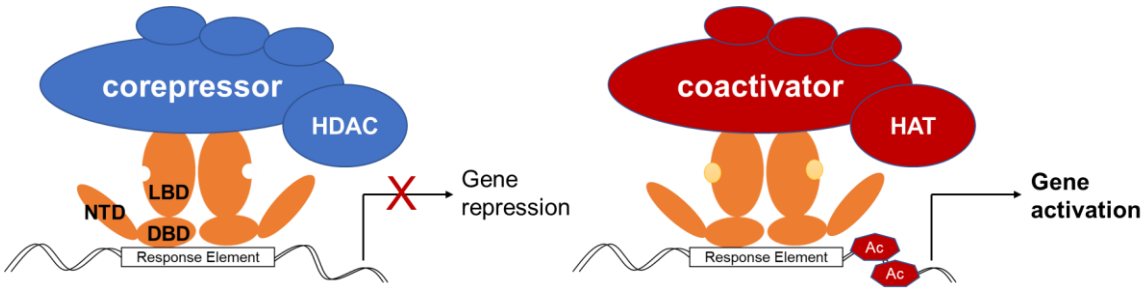

Figure 5. Schematic representation of transcriptional machinery of NRs

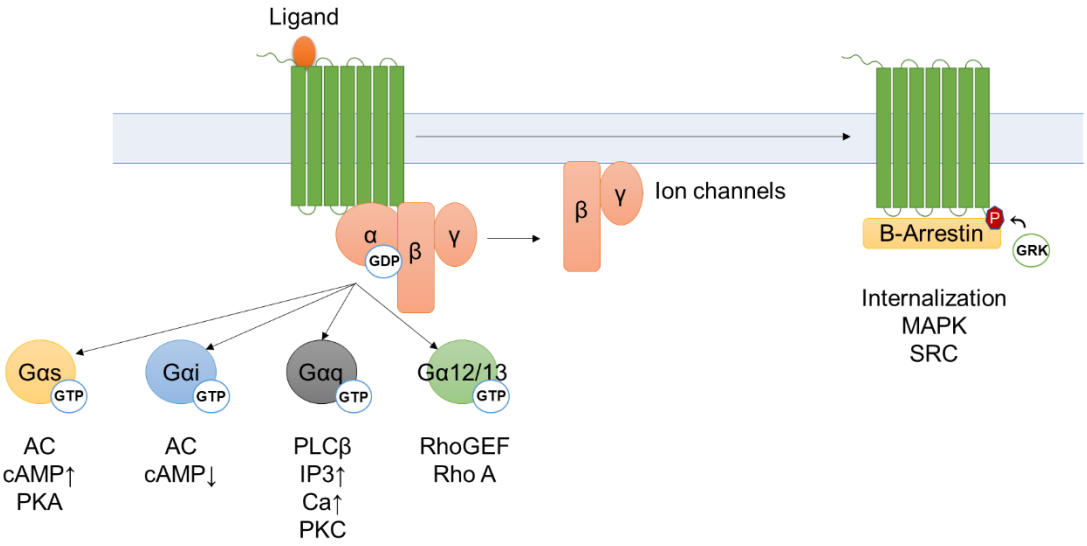

Figure 6. Schematic representation of GPCR signaling

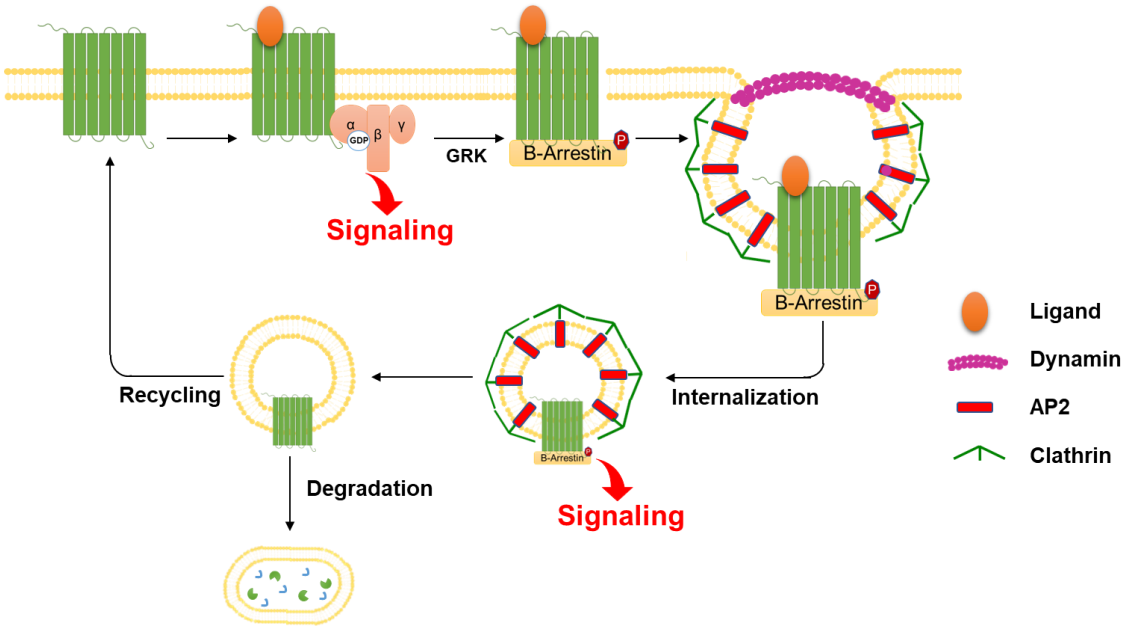

Figure 7. Schematic representation of GPCR trafficking

Chapter 1

Molecular mechanism of action of RORγt inverse agonist

Chapter 1　Molecular mechanism of action of RORγt inverse agonist

Abstract

The retinoic acid-related orphan receptor gamma t (RORγt) plays an important role in Th17 cell proliferation and functionality. Thus, RORγt inverse agonists are thought to be potent therapeutic agents for Th17-mediated autoimmune diseases, such as rheumatoid arthritis, asthma, inflammatory bowel disease, and psoriasis. Although RORγt has constitutive activity, the receptor is known to be physiologically regulated by various cholesterol derivatives. In this study, to identify RORγt inverse agonists through a HTS campaign, I compared an apo-RORγt protein from *Escherichia coli* and a cholesterol-bound RORγt protein from insect cells. As a result, the IC_{50} of the known RORγt inverse agonist TO901317 was markedly lower for the apo-protein than for the cholesterol-bound RORγt. Through HTS using a fluorescence-based cholesterol (TopFluor cholesterol) binding assay with the apo-protein, I identified Compound 1 as a novel cholesterol-competitive RORγt inverse agonist. Compound 1 inhibited the RORγt-TopFluor cholesterol interaction, coactivator recruitment, and transcriptional activity of RORγt. Cell-based reporter gene assay demonstrated that Compound 1 showed higher potency by lipid depletion treatment. Collectively, my findings imply that eliminating cholesterol from the RORγt protein is suitable for sensitive HTS to identify RORγt inverse agonists.

Introduction

RORα, β, and γ constitute a subfamily of the NR superfamily [24]. As an isoform of RORγ, RORγt shares identical DBD and LBD sequences with RORγ [25]. RORγt is expressed in several immune cell types, such as CD4+ Th17 cells, and is necessary for the proliferation and functionality of Th17 cells [26]. Th17 cells produce IL-17, which expression is generally increased responsive to pathogenic bacteria and fungi on mucous membranes, but excessive IL-17 expression inducing tissue inflammation is linked to various autoimmune diseases such as psoriasis, psoriatic arthritis, rheumatoid arthritis and multiple sclerosis [27, 28]. IL-17 expression is induced by RORγt, which directly binds to ROR response elements (ROREs) in the IL-17 promoter [29]. Hence, the differentiation of naive CD4+ T cells to Th17 cells is predominantly regulated by RORγt [30, 31]. Considering that antibodies against IL-17A or IL-17 A receptor are used for the treatment of psoriasis, psoriatic arthritis, rheumatoid arthritis [32], selective inactivation of the RORγt/IL-17 axis represents a promising therapeutic option for the treatment of autoimmune diseases. The LXR agonist, TO901317 (Fig. 8), has been identified as a potent RORγ inverse agonist [33]; since then, many inverse agonists have been identified, with some reportedly inhibiting Th17 cell differentiation. Among these compounds, SR1001, ursolic acid, and digoxin have been found to suppress experimental autoimmune encephalomyelitis [34]. These recent reports strongly suggest that RORγt is a potential target for autoimmune diseases.

Identification of endogenous ligands of RORs has been one of research interests. X-ray crystal structure analysis has unexpectedly revealed that cholesterol was present in the LBP of RORα protein purified from insect cells [35]. On the other hand, from the crystal structure of the RORβ protein expressed in *E. coli*, stearic acids were identified as a fortuitous ligand [36]. As to RORγ, the crystal structure of the LBD expressed in bacteria with a peptide motif of coactivator SRC-1 and hydroxycholesterols has been solved [37]. These structures information showed that the RORs in complex possess active conformations that generate a hydrophobic coactivator binding surface. Recently, several oxysterols were found to be agonistic ligands of RORγ and enhanced IL17 production in mice [38-42], suggesting that cholesterol biosynthetic intermediates may modulate the transcriptional activity of RORγ and RORγt.

The selection of the appropriate recombinant protein is necessary for more sensitive assays for HTS. To date, limited reports exist about the relationship between the ROR protein and cholesterol. In 2002, Kallen *et al*. reported that the RORα protein purified from Sf-9 cells was bound to cholesterol [35]; however, the protein expressed in *E. coli* yielded only insoluble protein. They presumed that cholesterol, which was reportedly not synthesized in the bacteria, was indispensable for stabilizing the receptor. In addition, they reported that cholesterol could be exchanged with cholesterol sulfate in the RORα protein, and the exchange of bound cholesterol sulfate could not be reversed with the excess of other cholesterol derivatives. In contrast, Wang

et al. showed that the RORα protein expressed in *E. coli* could be reconstituted in a lipid-free environment and had the ability to bind coactivator peptides [42]. The author also revealed that the RORα protein treated with excess cholesterol sulfate obstructed the binding of radiolabeled hydroxycholesterol to the receptor. From these reports, it was uncertain which host systems are appropriate for ROR protein production, and whether the relationship between cholesterol and the recombinant RORα protein is applicable to RORγt remains unclear. In addition, there is no evidence of the effect of cholesterol on RORγt inverse agonist activity.

The objective of this study described in Chapter 1 is to clarify the relationship of RORγt and cholesterol, and to identify novel RORγt inverse agonists through HTS. First, I revealed that cholesterol within the LBP of the recombinant RORγt protein interferes with the potency of RORγt inverse agonist. By utilizing this result, I conducted the HTS with a novel TopFluor cholesterol binding assay resulted in the identification of Compound 1 as a novel RORγt inverse agonist. TAK-828F, which was identified through further optimization of Compound 1, has higher potency, and selectivity against NRs, including ROR isoforms [43]. The compound also inhibited IL-17 secretion from mouse splenocytes and human primary cells, and inhibited Th17 cell differentiation from naive T cells and memory CD4+ T cells [44]. Furthermore, the compound showed significant efficacy in naive T cell transfer mouse colitis model [45].

Materials and Methods

Materials

TO901317 was purchased from Tocris Bioscience (Bristol, UK). Lovastatin and Cholesterol were purchased from FUJIFILM Wako Pure Chemical Corporation (Osaka, Japan). Cholesterol-sulfate was purchased from Sigma-Aldrich Corporation (St. Louis, MO).

Establishment of stable cell lines for reporter gene assay

The reporter-gene construct, pGL4.28-hIL17-ROREx3-luc, was constructed as described by Ichiyama, *et al*., [46]. Briefly, the construct was created by inserting an oligonucleotide, comprised of three copies of the ROR response element in the human IL17 promoter, into the pGL4.28 [luc2CP/minP/Hygro] reporter vector (Promega Corporation, Fitchburg, WI). The full-length cDNA for hRORγt was subcloned into the mammalian expression vector pMCMV-neo, which contained the cytomegalovirus promoter, to generate pMCMVneo-hRORγt. To generate stable cell lines, pGL4.28/hIL17-ROREx3-luc and pMCMVneo-hRORγt were transfected into the Jurkat Tet-On cell line (Takara Bio Inc, Kusatsu, Japan) using Gene Pulser (Bio-Rad Laboratories, Inc. Hercules, CA) and stable cell lines were chosen based on luciferase activity.

Protein expression and purification

The DNA fragment of human RORγt LBD (Uniprot: P51449, aa. 261-518), amplified by PCR, was cloned into the pFastBacHTb vector (Thermo Fisher Scientific, Waltham, MA). Recombinant baculovirus was generated using the Bac-to-Bac baculovirus expression system (Thermo Fisher Scientific). Protein expressed in Sf9 insect cells was harvested 48 h post-infection. Cell pellets were homogenized in lysis buffer [50 mM Tris-HCl, pH 7.9, 200 mM NaCl, 5% glycerol, 0.25 mM TCEP, and Complete™ protease inhibitor cocktail (Roche Diagnostics, Basel, Switzerland)]. Cell lysates were clarified by high-speed centrifugation at 37,000× g for 45 min and applied to affinity chromatography with ProBond Ni-chelating resin (Thermo Fisher Scientific). After extensive washing, the His-tagged protein was eluted by 50 mM Tris-HCl, pH 7.9, 150 mM NaCl, 200 mM imidazole, and 1 mM TCEP. The protein was then buffer-exchanged into 25 mM Tris-HCl, pH 8.0, 50 mM NaCl, 1 mM DTT, 1 mM TCEP before loading onto a MonoQ column (GE Healthcare, Chicago, IL). The flow-through fraction containing the LBD was collected. Protein concentration was measured using a NanoDrop spectrophotometer (Thermo Fisher Scientific). The purity of the protein sample was verified by SDS-PAGE and liquid chromatography mass spectrometry (Micromass LCT™ workstation, Waters Corporation, Milford, MA). A truncated human RORγt LBD (aa. 261-508) with an N-terminal 6xHis tag, followed by a TEV protease cleavage site, was cloned into a modified pET vector and expressed in *E. coli* BL21 (DE3) cells. The bacterial culture was grown in LB media at 37°C. When the culture reached an OD600 of 0.8, the cells were induced with 0.8 mM IPTG for an additional 18 h growth at 16°C before harvesting. The cell pellet was resuspended and sonicated in lysis buffer [25 mM Tris-HCl, pH 7.6, 1 M NaCl, 10 mM imidazole, 0.5 mM TCEP, 20 U/mL benzonase, 1 mg/ml lysozyme, and Complete™ protease inhibitor cocktail (Roche Diagnostics)]. The cell lysate was clarified by centrifugation (37,000× g, 45 min, 4°C) and applied to a 5 mL HiTrap Talon column (GE Healthcare). After an extensive wash, the His-tagged protein was eluted from the column with buffer containing 300 mM imidazole in 25 mM Tris-HCl, pH7.6, 1 M NaCl, 2 mM benzamidine, and 0.5 mM TCEP. The protein sample was buffer exchanged into 25 mM Tris-HCl, 200 mM NaCl, 2 mM benzamidine, 2 mM DTT, and 5% glycerol. It was then concentrated and loaded onto a size exclusion chromatography column (Hiload 16/60 Superdex 200, GE Healthcare). Peak fractions containing the truncated LBD protein were pooled and concentrated to 1 mg/ml. The purity of the final protein sample was verified by SDS-PAGE and LC-MS.

Quantification of cholesterol by mass spectrometry

Protein samples were dissolved in 0.5% SDS solutions to a concentration of 500 nM, and were heated at 95°C for 5 min to denature the sample completely. For this experiment, a Shimadzu HPLC system (Shimadzu Corp., Kyoto, Japan) and API 5000 triple quadrupole mass spectrometer (AB SCIEX, Framingham, MA) were used to quantify the concentration of cholesterol. The

analysis of cholesterol was performed using a Unison UK-C8 30 mm × 3 mm ID column, 3 μm (Imtakt, Kyoto, Japan). The HPLC mobile phase A contained 10 mM ammonium acetate in water, while mobile phase B contained 10 mM ammonium acetate in acetonitrile. The chromatographic separation of cholesterol was conducted using a constant ratio of 93% of mobile phase B in mobile phase A at a flow rate of 0.8 mL/min. According to the previous report for determination of 7α-OH cholesterol, the [M+H]+ ions are instable at high temperature in ionization step, and its daughter ions losing a water molecule are more stable20. So, the concentration of cholesterol was determined with selected monitoring methods and precursor ion scanning of m/z 369.3 (in a form of [M+H-H2O]+) in positive ion mode specific for cholesterol. The concentration of RORγt proteins were measured by Bradford Protein assay (Bio-Rad).

Reporter gene assay

The principle of the assay is outlined in Fig. 9A. Stable Jurkat cells were maintained in RPMI 1640 medium (Thermo Fisher Scientific) containing 10% FBS, 100 U/mL penicillin G, and 100 μg/mL streptomycin sulfate (Thermo Fisher Scientific). In experiments, cells were plated in 384-well white tissue culture plates (3570, CORNING Incorporated, Corning, NY) with 1 μg/mL of doxycycline (Takara Bio) at a density of 20,000 cells/well. For cholesterol depletion treatment, cells were maintained on RPMI 1640 containing 10% lipid reduced FBS (GE Healthcare) and 10 μM Lovastatin. Diminishing intracellular cholesterol was confirmed using Cholesterol Fluorometric Assay Kit (Cayman, Ann Arbor, MI) (data not shown). After culturing for 3 h, cells were treated with DMSO or test compounds and incubated at 37°C for 20 h. Luciferase activity was measured by Envision (PerkinElmer, Waltham, MA) using the Bright-Glo luciferase assay system (Promega). The cells treated with 1 mg/mL doxycycline were used as a high control, while the cells without doxycycline were used as a low control. Data were analyzed using Prism 5 (GraphPad Software, San Diego, CA), and a three-parameter logistic fit equation (Eq. (1)) was used to determine IC_{50}.

$Y = (Top - Bottom) / (1 +10^(X-LogIC_{50})) + Bottom$ Eq. (1)

“X” is the log of compound concentration, “Y” is the % of control. “Y” starts at “Bottom” and goes to “Top” with sigmoid shape.

TopFluor cholesterol/RORγt LBD (TR-FRET) binding assay screening

The principle of the assay is outlined in Fig. 9B. In 384-well black low-volume plates (Greiner Bio-One, Kremsmünster, Austria), 3 μL/well of the library compounds diluted with assay buffer [20 mM Tris-HCl (pH7.5), 100 mM NaCl, 1 mM DTT, 0.1% BSA] were added to a concentration of 1 μM. Final DMSO concentration was 1%. The plates were then incubated at room temperature for 20 min after the addition of 3 μL/well of hRORγt (*E. coli*) at a final concentration of 60 nM.

TopFluor cholesterol (3 μM, Avanti Polar Lipids, Alabaster, AL) and anti-His Tb (2 nM, Thermo Fisher Scientific) were then added to each well at 3 μL/well. An HT station 1200 (MSTechnos, Tokyo, Japan) was used to transfer the compounds, and a Multidrop Combi (Thermo Fisher Scientific) was used to transfer the hRORγt protein, TopFluor cholesterol, and anti-His Tb. The plates were incubated at room temperature for 1 h and measured in Envision. In order to eliminate false positive compounds, a Fluorescein-His Tag (2 nM, Thermo Fisher Scientific) was used instead of the hRORγt protein and TopFluor cholesterol. The Tb donor was excited at 320 nm, its emission was monitored at 486 nm, and the acceptor emission was monitored at 520 nm. The results were expressed as a ratio of Em520/Em486. The percent of inhibition was calculated based on wells containing DMSO as a high control and wells containing 10 μM of TO901317 as a low control. IC_{50} values were calculated in Eq. (1) using Prism 5.

Cell-free cofactor peptide recruitment assay

The principle of the assay is outlined in Fig. 9C. The binding of a cofactor peptide motif to the purified hRORγt protein was determined using the AlphaScreen Histidine (Nickel Chelate) Detection Kit (PerkinElmer). The experiments were conducted with 50 nM RORγt LBD and 10 nM of biotinylated SRC1-2 peptide (CPSSHSSLTERHKILHRLLQEGSPS, Scrum, Tokyo, Japan) in the presence of 10 μg/mL donor and acceptor beads in buffer containing 50 mM Tris-HCl (pH7.4), 50 mM KCl, 1 mM DTT, and 0.1% bovine serum albumin. Assay plates were incubated for 3 h at room temperature and measured by Envision. For normalization of the data in Table 2, wells containing DMSO were used as 100% controls and wells without the hRORγt protein were used as 0% controls. IC_{50} values were calculated Eq. (1) using Prism 5.

Thermal shift assay

In 96-well V-bottom polypropylene microplate (3363, CORNING), 20 μL/well of the test compounds dissolved in assay buffer [20 mM Tris-HCl (pH7.5), 100 mM NaCl, 1 mM DTT] were added with 20 μL/well of the RORγt protein expressed from *E. coli* (3 μM) and 20 μL/well of SYPRO Orange (500-fold diluted, Thermo Fisher Scientific). Then, 8 μL/well of the reaction were transferred to a 384 well PCR plate in quadruplicate. After centrifuging, the plates were heated at a ramp-rate of 1°C/min and the fluorescence was monitored by ABI 7900 (Thermo Fisher Scientific). Data were analyzed by Prism 5 (GraphPad Software), and Boltzman sigmoidal fitting was used to determine melting temperature (Tm).

Results

Molecular characterization of hRORγt proteins

To investigate the biological effect of a compound on NRs, cell-based reporter gene assay, cell-

free ligand binding assay, cell-free cofactor peptide recruitment assay are general assay methods [47]. Cell-based assays can measure transcriptional effect of a compound, however they detect a lot of false positive compounds such as toxic compounds or indirect regulators like kinase inhibitors. In contrast, cell-free assays are, although they do not exactly reflect the target in the cellular context, simple and detect few false positive compounds. So, I developed cell-free assay system for RORγt inverse agonist screening. In order to select the appropriate protein for primary screening, my colleague and I produced two types of human RORγt protein, expressed in *E. coli* [RORγt (*E. coli*)] and in insect cells [RORγt (Ins)]. Then I compared their differences regarding the presence of cholesterol in the LBD, ligand binding activity, cofactor recruitment activity, and tool compound effect.

At first, I performed mass spectrometry analysis for measuring the cholesterol content of the proteins. As a result, I found that more than 60% of the RORγt (Ins) protein contained cholesterol. In contrast, the RORγt (*E. coli*) protein did not contain any cholesterol, although there was a possibility that the protein would contain cholesterols incorporated from the medium during the cultivation of *E. coli* cells (Table 1). Furthermore, I compared the activity of these proteins using the TopFluor cholesterol competition assay (Fig. 9B) and cofactor recruitment assay (Fig. 9C). It was reported that RORγt was constitutive active and could interact with coactivator such as SRC1 without ligands [37]. Therefore, I used cell-free cofactor recruitment assay to determine whether the RORγt protein are active or inactive state by detecting interaction of SRC1-2 peptide with the RORγt LBD. I revealed that both RORγt (*E. coli*) and RORγt (Ins) proteins were effective in recruitment of the SRC1-2 peptide motif (Fig. 10A). Exogenous cholesterol weakly promoted to the SRC1 peptide recruitment by RORγt (*E. coli*) and the EC_{50} was about 2.5 μM, while its activation was not observed in reporter gene assay (data not shown). This observation implies that cholesterol is a very weak agonist not affecting transcriptional activity of RORγt. To investigate cholesterol binding activity of these proteins, I developed TR-FRET binding assay, which detects TopFluor cholesterol binding to the RORγt LBD. As shown in Fig. 10B, the RORγt (*E. coli*) protein could specifically bind TopFluor cholesterol compared to no protein control and the apparent K_d was calculated as 6.3 μM. Whereas, the binding of the RORγt (Ins) was only detected at less than 10% of the RORγt (*E. coli*) binding capability. Exogenous cholesterol can displace the TopFluor cholesterol in RORγt (*E. coli*) LBD and its IC_{50} was about 7.2 μM.

I then examined whether differences in host cells alter the potency of the inverse agonist activity using TO901317, which is a known RORγt inverse agonist. I revealed that TO901317 was over 200-times more potent on RORγt (*E. coli*) (IC_{50} = 23 nM) than on RORγt (Ins) (IC_{50} = 6,700 nM) in SRC1-2 recruitment activity (Fig. 10C). Crystal structure of the ligand binding domain of RORγ with TO901317 showed that binding site of this compound is same as cholesterol binding site [48]. To corroborate this structural information, I conducted in TopFluor

cholesterol binding assay to confirm TO901317 is ligand competitive or not. As expected, the IC_{50} value of TO901317 was right-ward shifted dependent on increasing TopFluor cholesterol concentration (Fig. 10D). It is difficult to increase TopFluor cholesterol concentration more than 10 μM (about 2-fold higher than K_d) because of its solubility. This data demonstrates that TO901317 inhibited TopFluor cholesterol binding in a competitive manner. In order to determine whether the reason was due to the difference in expression system or the presence of cholesterol, I tested the activity of RORγt (*E. coli*) incubated with excess cholesterol sulfate and applied to gel-filtration to remove free cholesterol sulfate. Wang *et al*. used cholesterol sulfate for examining the effect of exogenous sterol to the RORα LBD [42]. Hence, I used cholesterol sulfate as a surrogate ligand because it had more solubility and higher affinity for RORγt (IC_{50} = 46 nM data not shown) than cholesterol and it is thought to be non-functional ligand like cholesterol in cofactor recruit assay and reporter gene assay according to previous report. Cholesterol sulfate-saturated RORγt (*E. coli*), as well as RORγt (Ins), blocked the binding of the Top-Fluor cholesterol (Fig. 10B) and inhibition by TO901317 in cofactor recruitment assay (IC_{50} > 10,000 nM, Fig. 10C), indicating that bound cholesterol sulfate is hardly exchanged from the RORγt protein. From these results, I selected the apo-RORγt (*E. coli*) protein for primary screening because it was expected that using the apo-protein would identify a greater variety of hit clusters of RORγt inverse agonists.

High-throughput screening

Among two established cell-free assays, I selected the TopFluor cholesterol competition assay for primary screening to pick not only inverse agonists, but also antagonists, which cancel the agonistic activity of cholesterol derivatives. TopFluor cholesterol concentration was set as 3 μM according to the apparent K_d from titration data (Fig. 10B) and assay robustness. I conducted an assay validation such as duplicate (N2) correlation and batch reproducibility, and set the test concentration as 1 μM based on a hit rate of prescreening (data not shown). Following the validation, I conducted a HTS on the 860,000 compounds of the Takeda compound library at 1μM as outlined in Fig. 11A. From a scatter plot of 1% DMSO treated controls and TO901317 treated controls in a single representative data from the primary screening (Fig. 11B), Z'-Factor was calculated as 0.86. The average Z'-factor of all plates tested was 0.80 ± 0.05 (average ± standard deviation) with an average plate S/B ratio of 10.80 ± 1.23. The primary screening data in histogram format (Fig. 11C) showed a normal distribution curve with an average inhibition value of 10.9% and a standard deviation of 17.2%. The remaining compounds above 70% at 1 μM from primary screening were tested in the counter assay using a Fluorescein-His tag to eliminate false positive compounds due to the inhibition of the TR-FRET signal. In total, 229 compounds passed the counter assay, and from these, 68 compounds showed >70% inhibition against the apo-RORγt-

SRC1 peptide interaction at 1 μM. Following RORγt-RORE reporter gene assay, I identified 23 clusters (41 compounds) as hit compounds. Of these hit compounds, Compound 1 (Fig. 11D) was selected as a lead compound because the compound had 15-fold greater selectivity against RORα and RORβ (data not shown), has good physical properties including water solubility and cLogP of 2.8, and did not have cytotoxicity and CYP inhibition. Table 2 shows the IC_{50} values of Compound 1 and TO901317 for RORγt in three functional assays. Compound 1, similar to TO901317, was effective in the TopFluor cholesterol binding assay (IC_{50} = 200 nM), the SRC1-2 recruitment assay (IC_{50} = 91 nM), and the RORγt-RORE reporter gene assay (IC_{50} = 1,600 nM), although the potency of Compound 1 was slightly weaker than TO901317. To confirm the direct interaction between Compound 1 and RORγt, I performed TSA. TSA is a common method to confirm direct binding of small molecule to the target protein including RORγ [38, 49]. TSA monitors the thermal stability of the target protein with fluorescent dye such as SYPRO Orange, which emit fluorescence when hydrophobic residues of the protein are exposed to the dye. A ligand induced conformational stabilization of the target protein can be judged by comparing Tm with or without ligands. As shown in Fig. 12A and 12B, Tm value of TO901317 (51.6°C at 30 μM) and Compound 1 (51.7 °C at 30 μM) were higher than that of the apo-form of RORγt (*E. coli*) (Tm = 45.3°C). Tm shift by Compound 1 at 3 μM (2.4°C) was lower than by TO901317 (3.6°C) consistent with their order of IC_{50} in cell-free assay. Thus, I confirmed the direct binding of Compound 1 in TSA.

The effect of cholesterol on the potency of Compound 1 in cell-free and cell-based assay

To evaluate the effect of cholesterol on the inhibition of Compound 1, I conducted cell-free SRC1-2 recruitment assay and cell-based reporter gene assay. In SRC1-2 recruitment assay, similar to TO901317, the IC_{50} of Compound 1 was over 100-times lower for apo-RORγt (*E. coli*) than for RORγt (Ins) and cholesterol sulfate-bound RORγt (*E. coli*) (Fig. 13A). These results revealed that Compound 1 could not have been identified if RORγt (Ins) was used for primary screening. Fig. 13B showed that Compound 1 inhibited Top-Fluor cholesterol binding of RORγt protein in a competitive manner as same as TO901317, and further structural analysis of Compound 1 derivative revealed that this chemotype bind to cholesterol binding site [50]. To confirm the effect of cholesterol on the RORγt transcriptional activity, I used RORE reporter gene assay (Fig. 9A) detecting an inhibitory effect on the RORγt's constitutive active transcriptional activity by the inverse agonist. Compound 1 was then tested with normal medium, cholesterol-depleted medium (lipid-reduced FBS and 10 μM of Lovastatin), or cholesterol-depleted medium containing cholesterol sulfate. First, I clarified that cholesterol depletion and Cholesterol sulfate treatment had almost no effect against RORγt transcriptional activity suggesting that cholesterol and cholesterol sulfate are non-functional ligands (Fig. 13C). Second, I showed that the IC_{50} value

of Compound 1 was 3.1 μM with cholesterol depletion treatment, which was lower than the IC_{50} value of 14 μM without cholesterol depletion (Fig. 13D). Finally, I revealed that increasing amounts of cholesterol-sulfate in the cholesterol-depleted medium induced a rightward IC_{50} shift, although the transcriptional activity without Compound 1 did not increase with cholesterol-sulfate. These results strongly suggest that the IC_{50} shift in the inverse agonist activity by lovastatin was caused by the intracellular cholesterol concentration, not an indirect effect of lovastatin. From these results, I concluded that, in cell-free assay, TO901317 and Compound 1 bind to LBP of apo-RORγt protein inducing inactive form resulted in inhibiting the recruitment of SRC-1 peptide, while cholesterol bound RORγt protein was hardly exchanged by these RORγt inverse agonists and sustained active form with the recruitment of SRC1 peptide (Fig. 14). Furthermore, in cell-based assay the intra-cellular cholesterol level affected the potency of the RORγt inverse agonist. As is evident from these data, reducing cholesterol levels in both cell-free and cell-based assay is necessary for the sensitive screening of RORγt inverse agonists.

Discussion

By using cell-free assays, I have shown that TO901317 was more potent on the RORγt (*E. coli*) protein than on the RORγt (Ins) protein due to the difference in their cholesterol content. In addition, I identified Compound 1 as a novel RORγt inverse agonist through HTS with the apo-RORγt protein. In cell-based reporter gene assay, reducing intra-cellular cholesterol levels lowered the IC_{50} of Compound 1. Although the apo-RORγt protein expressed in *E. coli* was already used in cell-free functional assays, and cholesterol depletion treatment has been used in cell-based assays by different authors [38, 42], the results obtained in the present study show the effect of cholesterol on the potency of RORγt inverse agonists is large. Thus, excluding cholesterol is important for sensitive assays in order to conduct HTS. In fact, HTS using SRC1-2 recruitment assay with a small-scale library with the RORγt (Ins) protein yielded no positive compounds (data not shown).

Although the data using LC/MS showed that approximately 60% of RORγt (Ins) is bound to cholesterol, Topfluor cholesterol could bind less than 10% of the RORγt (Ins). This discrepancy is thought to be attributed to the presence of other cholesterol derivatives because I detected the specific peak for cholesterol. This observation is consistent with the report by Bitsch F *et al*. showing that 77% of cholesterol and 18% of 7-dehydrocholesterol were bound with RORα LBD protein expressed in Sf9 cells [51]. For the recombinant protein production, a variety of expression hosts are used including bacteria, mammalian cells, yeast, and insect cells [52]. Among them, the most historical system is the bacteria *E. coli* because of low cost, ease of use, and availability of expression vectors [53]. On the other hand, baculovirus expression system is also used to produce the recombinant protein requiring post-translational modification such as folding,

phosphorylation, and glycosylation [54]. The commonly used insect cell lines for this system are derived from Spodoptera frugiperda (Sf9 and Sf21). I revealed that the RORγt (*E. coli*) protein is apo-protein without cholesterol, which is probably due to absent cholesterol synthesis system in bacteria. Therefore, my results suggest that considering ligand metabolism in each host is required for appropriate recombinant NR protein expression.

As for the cell-free assay, we showed that Compound 1 and TO901317 could not exchange the endogenous cholesterol bound to the RORγt protein (IC_{50} of Compound 1 was >10 μM). While in cell-based RORγt reporter gene assay, they inhibited RORγt transcriptional activity (IC_{50} of Compound 1 was 14 μM) in normal FBS medium in which intracellular cholesterol is abundant and IC_{50} ratio of normal condition vs cholesterol depletion treatment in reporter gene assay was lower than cell-free assay. In addition, various inverse agonist compounds including ursolic acid, and digoxin are effective *in vivo* assay although endogenous cholesterol is present [55] suggesting that LBP of RORγt in mammalian cells is exchangeable by inverse agonists. I speculated one reason that the intracellular turn-over of RORγt is faster than that of other cellular proteins. In fact, our SILAC analysis showed that the half-time of RORγt was approximately 6.2 h (data not shown). On the time scale of the cell-based assay, RORγt inverse agonists and cholesterol may compete for the binding site of RORγt protein newly generated in the cell body. Another possible reason is that cholesterol derivatives bound to RORγt in mammalian cells can be exchanged by the inverse agonists because of weaker affinity. These observation in which ligand bound with purified protein act as a potency tuner is supported by the previous reports with HNF4 family, which show high constitutive activity. Crystallographic analysis of HNF4α and HNF4γ LBD protein identified a mixture of fatty acids [56, 57] and the endogenous fatty acids bound with the recombinant protein did not readily exchange with radiolabeled palmitic acid. On the other hand, affinity isolation/mass spectrometry showed that endogenously expressed HNF4α in mammalian cells was occupied by linoleic acid. This ligand was silent ligand and linoleic acid bound HNF4α protein was exchangeable by another ligand in mammalian cells. These reports suggest that composition of ligands bound with the NR protein are different in host cells, and further investigation of the factual form of the RORγt LBD in mammalian cells should be conducted.

In conclusion, I identified Compound 1 as a cholesterol-competitive RORγt inverse agonist, and showed that the potency of Compound 1 depends on whether the receptor is saturated with cholesterol or not. This study emphasizes the importance of characterizing the recombinant protein and the optimization of cell-based assay conditions for HTS and should impact the investigation of other orphan nuclear receptors for obtaining new lead compounds.

Figures and Tables

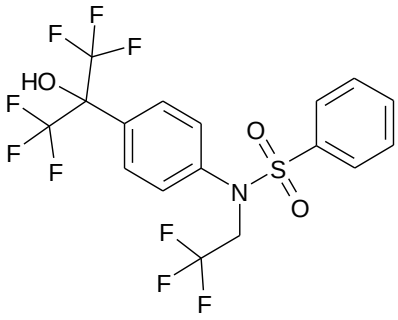

Figure 8. Chemical structure of TO901317

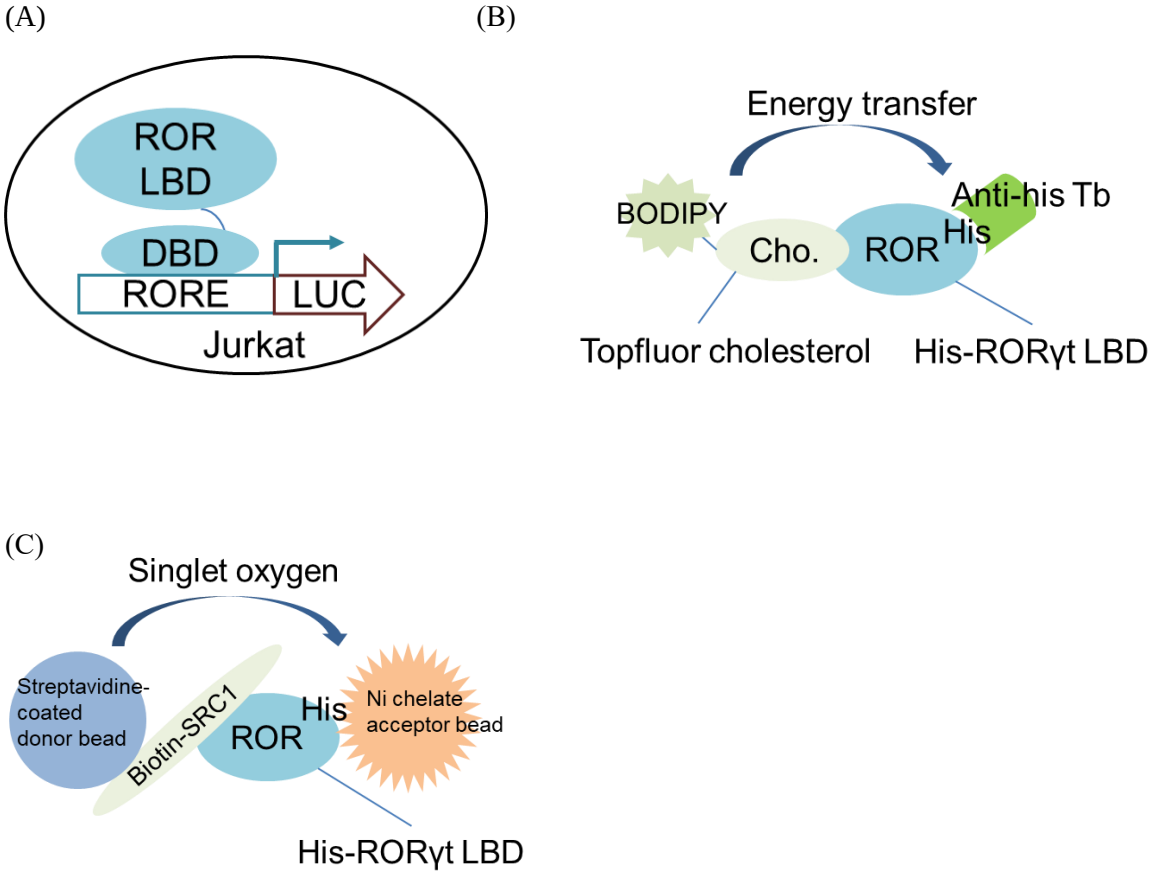

Figure 9. Assay principle of biochemical assay for analyzing RORγt function

(A) RORE reporter gene assay. (B) TopFluor cholesterol binding assay.

(C) Cofactor peptide recruitment assay.

(A)

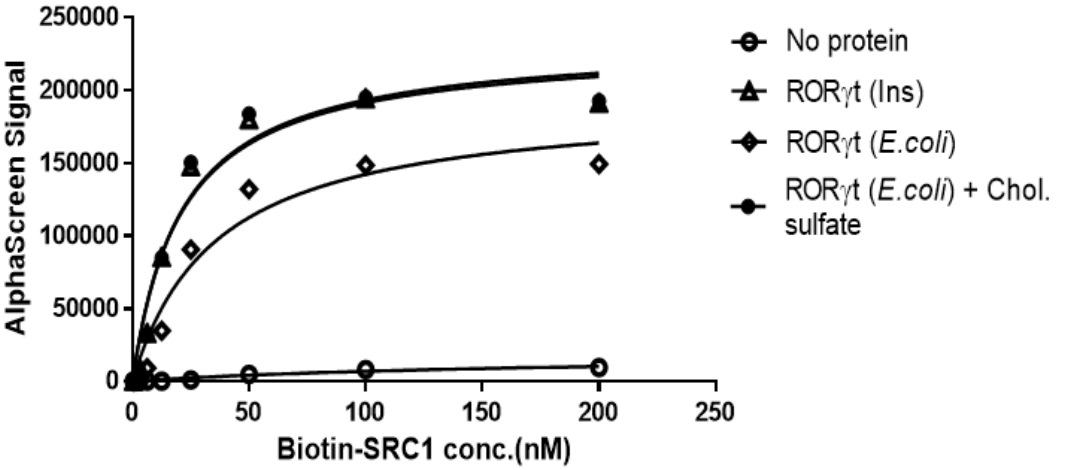
AlphaScreen Signal
250000
200000
150000
100000
50000
0
0
50
100
150
200
250
Biotin-SRC1 conc.(nM)
No protein
RORγt (Ins)
RORγt (E.coli)
RORγt (E.coli) + Chol. sulfate

(B)

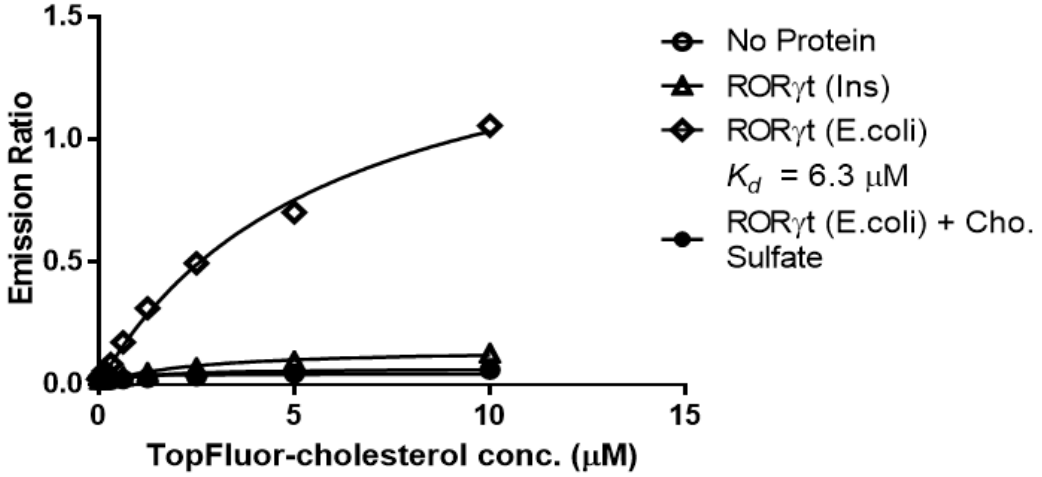
Emission Ratio
1.5
1.0
0.5
0.0
0
5
10
15
TopFluor-cholesterol conc. (μM)
No Protein
RORγt (Ins)
RORγt (E.coli)
K_d = 6.3 μM
RORγt (E.coli) + Cho. Sulfate

(C)

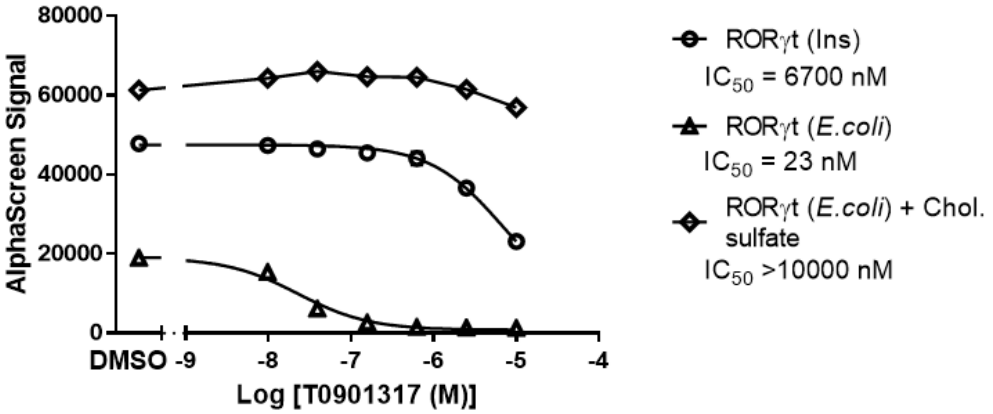

(D)

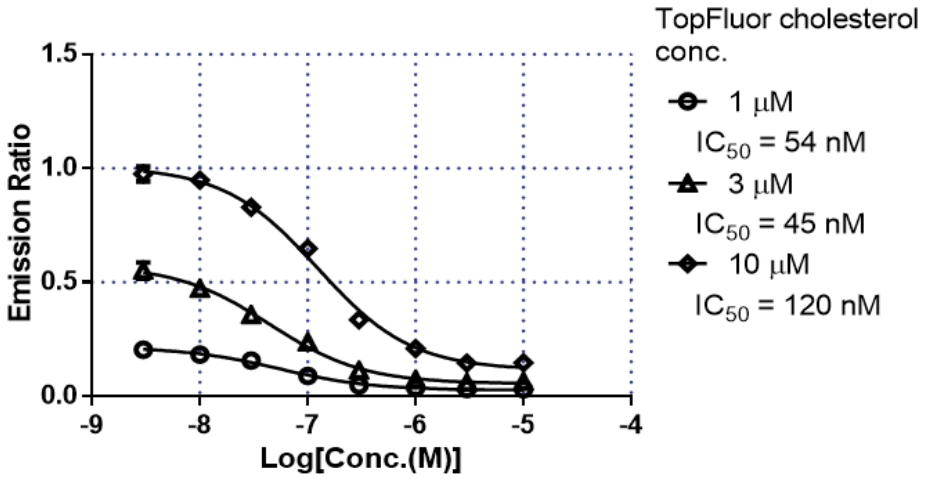

Figure 10. Cholesterol binding activity and SRC1-2 peptide recruitment activity of the three hRORγt proteins. hRORγt (Ins), hRORγt (*E. coli*), and cholesterol sulfate-saturated hRORγt (*E. coli*) were analyzed by cofactor peptide recruitment assay and TopFluor cholesterol binding assay. (A) The interaction of hRORγt (Ins) (△), hRORγt (*E. coli*) (◊), and cholesterol sulfate-saturated hRORγt (*E. coli*) (●) with the biotin-SRC1-2 peptide was monitored using AlphaScreen assay. Non-specific signals were detected without ROR proteins (○). Data are shown as the mean ± SEM of duplicate wells. (B) Binding of TopFluor cholesterol to hRORγt (Ins) (△), hRORγt (*E. coli*) (◊), and cholesterol sulfate-saturated hRORγt (*E. coli*) (●) was detected using the TR-FRET

system. Non-specific signals were detected without ROR proteins (○). Data are shown as the mean ± SEM of duplicate wells. K_d values were determined with GrahPad Prism 5 using a nonlinear regression method, a one-site fitting model. (C) The recombinant protein of RORγt (Ins) (○), hRORγt (*E. coli*) (△), and cholesterol sulfate-saturated hRORγt (*E. coli*) (◊) were incubated with 10 nM biotin-SRC1-2 peptide and various concentration of TO901317 for 3 h at room temperature. Data are shown as the mean ± SEM of duplicate wells. IC_{50} values were calculated as described as Materials and Methods by using raw data. (D) Inhibition of TopFluor cholesterol binding by TO901317 with 1 (○), 3 (△), or 10 μM (◊) TopFluor cholesterol. Data are shown as the mean ± SEM of duplicate wells. IC_{50} values were calculated as described in Materials and Methods without normalization of the data.

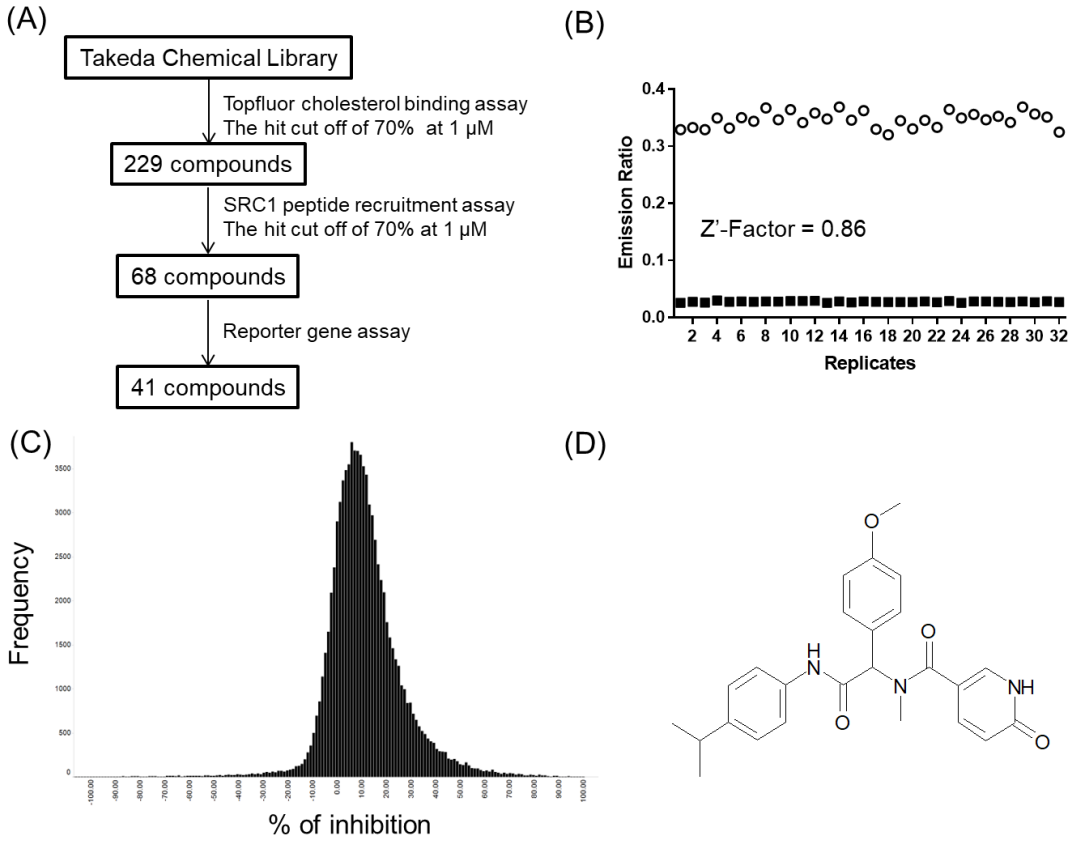

Figure 11. Primary screening results. (A) Flow chart of screen procedure. (B) Scatterplot of 1% DMSO controls (○) and 10 uM TO901317 + 1% DMSO controls (■) from a single representative data in primary screening. Z'-Factor was calculated from these 16 replicated controls using the TopFluor cholesterol-RORγt (*E. coli*) TR-FRET binding assay. (C) Histogram of % inhibition of the Takeda Library compounds from primary screening (D) Chemical structure of Compound 1.

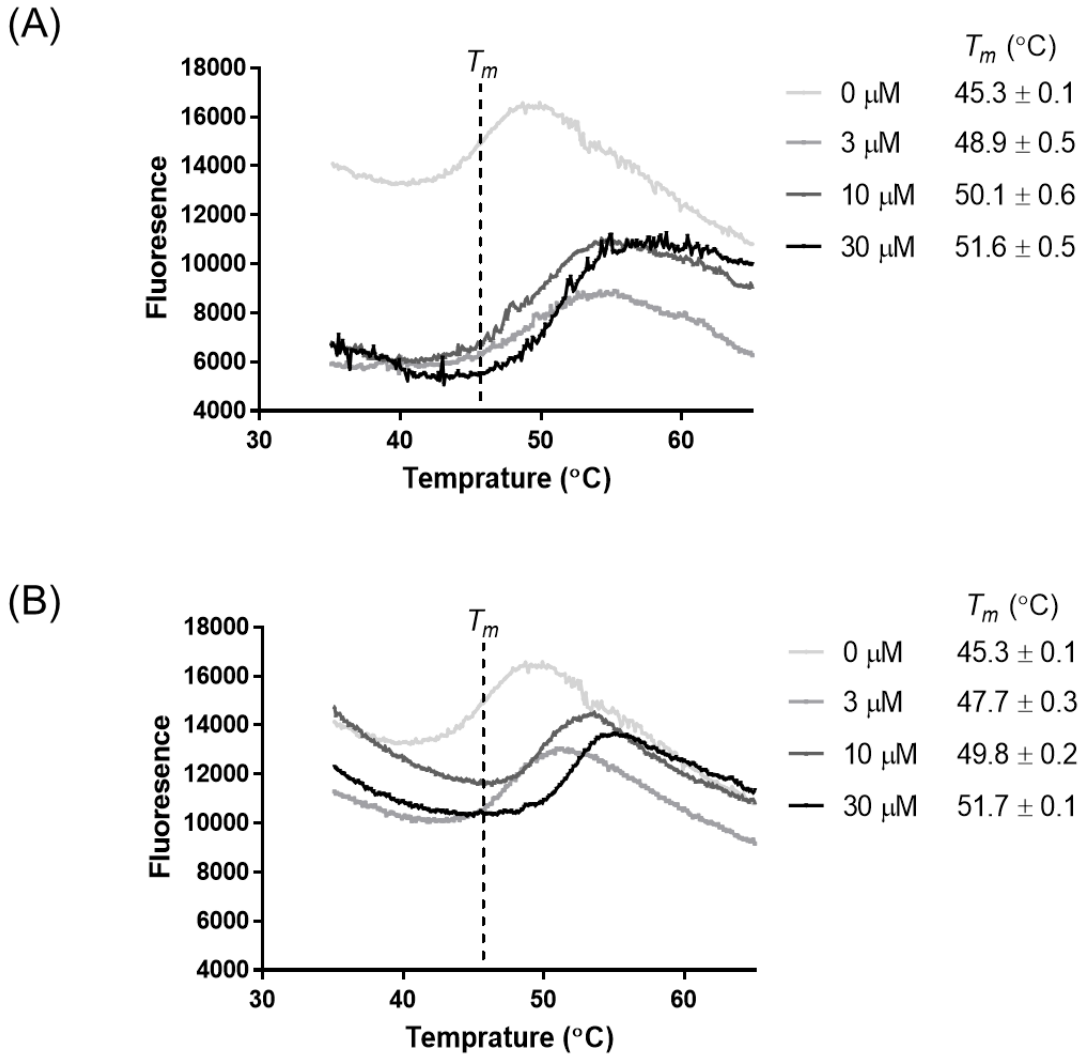

Figure 12. Thermal shift assay data of RORγt in the presence or absence of the RORγt inverse agonists. Representative melting curves of RORγt (*E. coli*) with 0, 3, 10, or 30 μM TO901317 (A) and Compound 1 (B) are shown with calculated Tm. Tm are reported as mean ± SD from three independent experiments (n = 4).

(A)

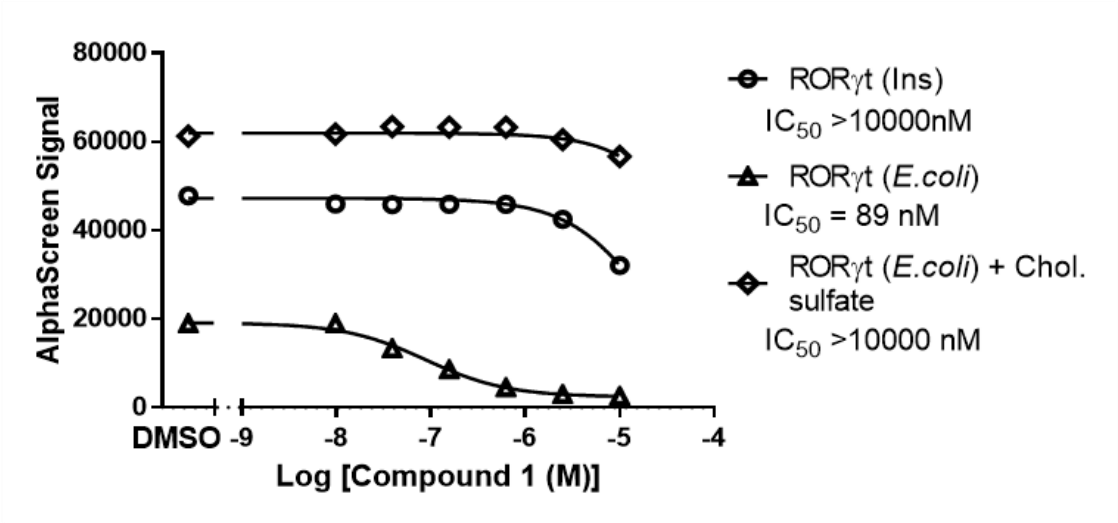
80000
60000
40000
20000
0
AlphaScreen Signal
DMSO
-9
-8
-7
-6
-5
-4
Log [Compound 1 (M)]
RORγt (Ins)
IC50 >10000nM
RORγt (E.coli)
IC50 = 89 nM
RORγt (E.coli) + Chol. sulfate
IC50 >10000 nM

(B)

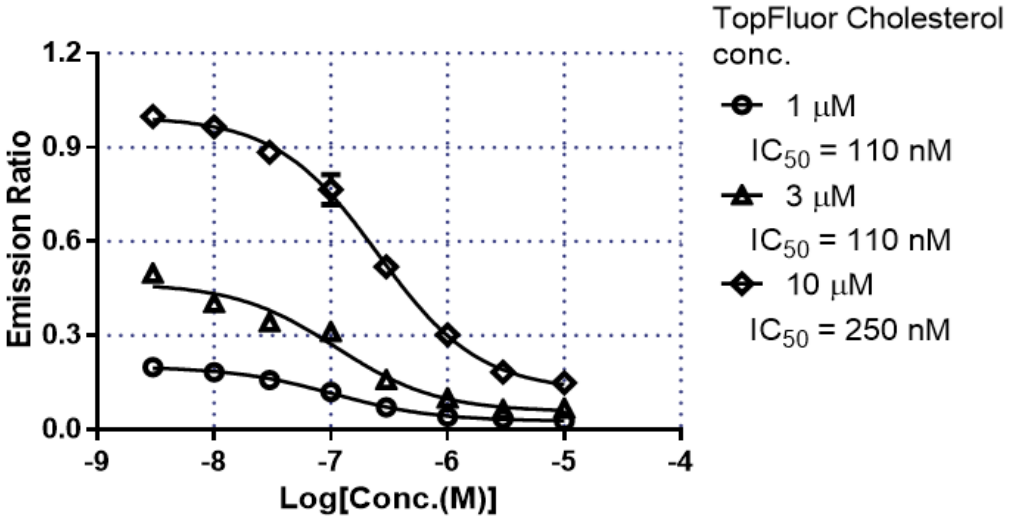
1.2
0.9
0.6
0.3
0.0
Emission Ratio
-9
-8
-7
-6
-5
-4
Log[Conc.(M)]
TopFluor Cholesterol conc.
1 μM
IC50 = 110 nM
3 μM
IC50 = 110 nM
10 μM
IC50 = 250 nM

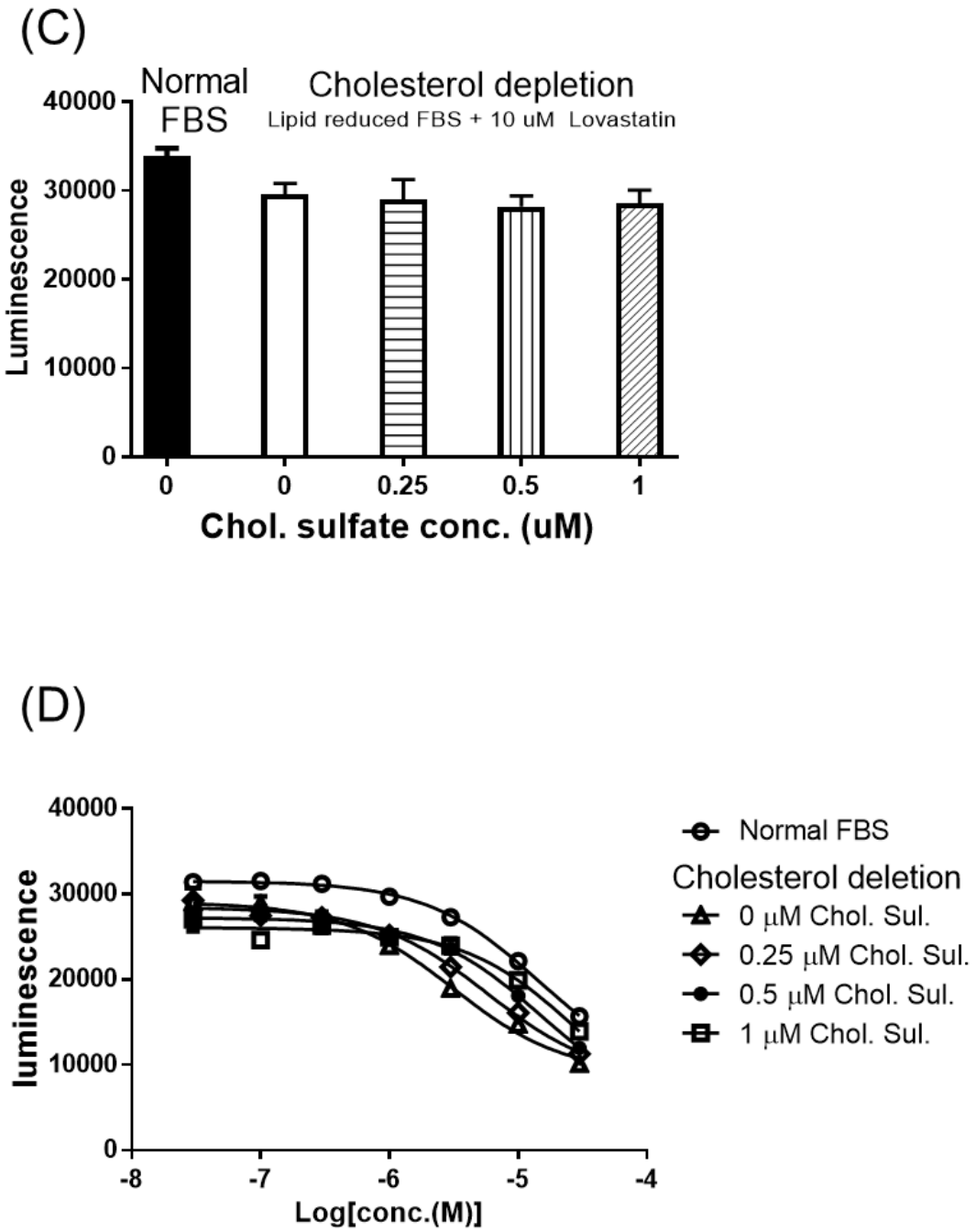

Figure 13. The effect of cholesterol on the potency of Compound 1 in SRC1-2 peptide recruitment assay and reporter gene assay. (A) The recombinant protein of RORγt (Ins) (○), hRORγt (*E. coli*) (△), and cholesterol sulfate-saturated hRORγt (*E. coli*) (◊) were incubated with 10 nM biotin-SRC1-2 peptide and various concentrations of Compound 1 for 3 h at room temperature. Data are shown as the mean ± SEM of duplicate wells. IC_{50} values were calculated as described in Materials and Methods without normalization of the data. (B) Inhibition of TopFluor cholesterol binding by Compound 1 with 1 (○), 3 (△), or 10 μM (◊) TopFluor cholesterol. Data are shown

as the mean ± SEM of duplicate wells. IC_{50} values were calculated as described in Materials and Methods without normalization of the data. (C) Effect of cholesterol depletion treatment and addition of cholesterol sulfate (starting at 1 μM; 1:2 serial dilutions) against RORγt transcriptional activity in cell-based reporter gene assay. The data are shown as the mean ± SD of duplicate wells. (D) The hRORγt stable cell line was incubated for 18 h with the indicated concentration of Compound 1 in medium containing normal FBS (○) or lipid-reduced FBS with 10 μM Lovastatin and 0 (△), 0.25 (◊), 0.5 (●), 1 uM (□) cholesterol sulfate. Data are shown as the mean ± SEM of quadruplicate wells. IC_{50} values were calculated as described in Materials and Methods without normalization of the data.

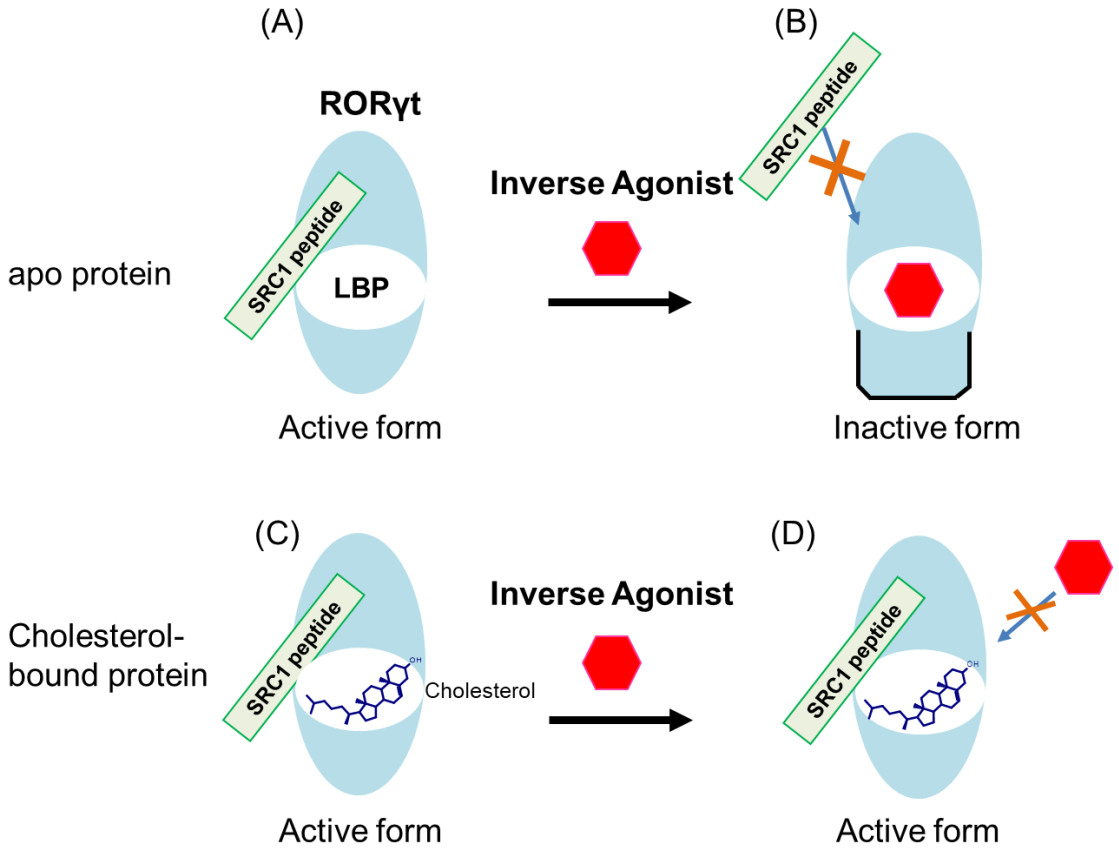

Figure 14. The effect of cholesterol against the recombinant hRORγt protein and hRORγt inverse agonist. Cholesterol-free apo protein has constitutive activity and can interact with SRC1 peptide (A). Cholesterol-competitive inverse agonists such as TO901317 and Compound 1 bind to the LBP inducing a conformational change, leading to a blockade of RORγt-SRC1 peptide interaction (B). Cholesterol-bound protein is an active form inducing the recruitment of SRC1 peptide (C). The inverse agonists seldom to replace the cholesterol in the LBP of cholesterol-bound protein, and the interaction between RORγt and SRC1 peptide are still sustained (D).

Table 1.

Cholesterol concentration in the hRORγt protein expressed in insect cells or *E. coli* as measured by mass spectrometry.

	Protein Conc. (nM)	Cholesterol Conc. (nM)	Bound Rate (%)
hRORγt expressed in insect cells	517	318	62
hRORγt expressed in *E. coli*	550	0	0

Table 2.

IC_{50} values of Compound 1 and T0901317 in RORγt reporter gene assay, TopFluor cholesterol binding assay, and cofactor recruitment assay using apo-RORγt (*E. coli*).

Compound	Topfluor cholesterol binding IC_{50} (95% CI) nM	SRC1 peptide recruitment assay IC_{50} (95% CI) nM	Reporter gene assay IC_{50} (95% CI) nM
Compound 1	200 (160–250)	91 (67–130)	1600 (1200–2200)
TO901317	91 (64–130)	23 (16–33)	1500 (1200–1900)

For reporter gene assay, compounds were tested in duplicate in medium containing lipid-reduced FBS with 10 μM Lovastatin. IC_{50} values were calculated as described in Materials and Methods using normalized data from a single experiment performed in duplicate. [CI = confidence interval]

Chapter 2

Molecular mechanism of action of GPR40 full agonist

Chapter 2 Molecular mechanism of action of GPR40 full agonist

Abstract

Full agonist-mediated activation of GPR40 alleviates diabetes in rodents. Given that diabetes is a chronic disease, assessment of treatment durability of chronic exposure to a GPR40 full agonist is crucial for treating patients with diabetes. However, the physiological significance of chronic *in vitro* and *in vivo* exposure to GPR40 full agonists is largely unclear. I evaluated the *in vitro* and *in vivo* effects of chronic treatment with SCO-267, a GPR40 full agonist, on signal transduction and glucose control. First, I showed that SCO-267 is an allosteric full agonist of GPR40, which activates the Gαq, Gαs, Gα12/13 pathways, and β-arrestin recruitment. Second, I revealed that the Gαq signal response was largely sustained in GPR40-overexpressing CHO cells even after prolonged incubation with SCO-267. Third, I evaluated the *in vivo* relevance of chronic exposure to GPR40 full agonists. SCO-267 (1 and 10 mg/kg) was administered once daily to N-STZ rats for 15–33 days, and glucose control was evaluated. After 15 days of dosing followed by the drug wash-out period, SCO-267 improved glucose tolerance most likely by increasing insulin sensitivity in rats. After 33 days, repeated exposure to SCO-267 was still highly effective in improving glucose tolerance in rats. Moreover, chronic exposure to SCO-267 increased pancreatic insulin content. These results demonstrated that even after chronic exposure, SCO-267 effectively activates GPR40 in cells and rats, suggesting the clinical application of SCO-267 in treating chronic diseases including diabetes.

Introduction

GPR40 is a GPCR that is endogenously activated by medium-to-long chain fatty acids [58, 59]. The receptor potentiates the secretion of glucose-dependent insulin from pancreatic β-cells and stimulates the secretion of incretins such as GLP-1 from intestinal endocrine cells [60, 61]. Fasiglifam, a partial agonist of GPR40, which improves glycemic control mainly by stimulating insulin secretion [62], showed a glucose-lowering effect in clinical studies on patients with T2DM [63, 64]. The results of these clinical trials imply that GPR40 is a promising therapeutic target for T2DM. Since the report of the superior glucose-lowering efficacy of a full GPR40 agonist, AM-1638, over a partial GPR40 agonist [65], various synthetic full GPR40 agonists have been investigated as new drug candidates [66, 67]. These full agonists bind to the allosteric binding site of the receptor distal from the binding sites for endogenous ligands or fasiglifam [65, 68, 69]. Furthermore, in contrast to the partial agonists activating the Gαq signal, these full agonists activate not only the Gαq signal but also the Gαs [70] and Gα12/13 signals [71], which may explain its robust incretin stimulation and maximal efficacy in preclinical models [72]. Based on these observations, GPR40 full agonists have been suggested as a novel strategy to treat diabetes [73].

Considering that diabetes is a chronic disease with metabolic dysfunctions, the durability of drug efficacy is highly important [74], and this is also the case with full agonists for GPR40. Generally, chronic agonist exposure causes GPCR desensitization and internalization, so the response is reduced [75, 76]. These effects occur within a few minutes to hours, depending on the GPCRs and agonist ligands. For example, relaxin family peptide receptor 1 demonstrates prolonged agonist-induced cAMP response by lack of β-arrestin interaction and poor internalization [77]. In addition, the neuropeptide FF-activated proto-oncogene MAS can be re-stimulated in calcium response, whereas the receptor activated by non-peptide ligands cannot be stimulated [78]. A durable glycemic control effect of GPR40 partial agonists in preclinical models has been reported [79, 80], and patients with T2DM treated with fasiglifam continued to exhibit reduced HbA1c for 52 weeks [64]. However, the *in vitro* and *in vivo* effect of chronic exposure to GPR40 full agonist on downstream signaling of GPR40 is still uncertain. Therefore, evaluating the downstream signaling of GPR40 upon chronic treatment with GPR40 full agonists is of importance when considering the application of this class of compounds for treating chronic metabolic diseases in clinical settings.

The aim of this study is to elucidate the *in vitro* and *in vivo* effect of chronic exposure to SCO-267, a GPR40 full agonist, on downstream signaling of GPR40. Using a recombinant expression system, I analyzed the signal transduction and allosteric properties of SCO-267. Furthermore, I investigated the chronic effect of SCO-267 with respect to the Gαq signal in cell models. Finally, I evaluated the chronic effects of SCO-267 on glycemic control in a rat model.

Materials and Methods

Materials

SCO-267, fasiglifam, and AM-1638 were obtained from SCOHIA PHARMA (Fujisawa, Japan). γ-Linolenic acid was purchased from Sigma-Aldrich (Tokyo, Japan). For *in vitro* studies, compounds were dissolved in dimethyl sulfoxide, except for γ-linolenic acid, which was dissolved in ethanol. For *in vivo* studies, compounds were suspended in 0.5% methylcellulose solution (FUJIFILM Wako).

IP1 HTRF assay for Gαq signaling

CHO dihydrofolate reductase-deficient cells stably expressing human FFAR1 (mRNA for GPR40) with different receptor mRNA expression levels were established previously [81]. The mRNA copy number in high (clone 104) and low (clone 2) FFAR1-expressing cells was quantified by quantitative polymerase chain reaction as reported previously. These cells were cultured in MEM-α (Thermo Fisher Scientific) supplemented with 10% dialyzed FBS (GE Healthcare), 100 U/ml penicillin–streptomycin (FUJIFILM Wako), and 10 mM HEPES solution (FUJIFILM Wako), and were tested for mycoplasma contamination before the experiment. The day before the assay, human FFAR1-expressing CHO cells were plated at 5000 cells per well in poly D-lysine-coated 384-well white plates. After culturing overnight, the cells were treated with compounds in stimulation buffer (included in the IP-One HTRF assay Kit; PerkinElmer) containing 0.01% fatty acid-free BSA at varying concentrations, and incubated at 37°C for 30 min. Intracellular IP1 level was measured using the IP-One HTRF Assay Kit (PerkinElmer) according to the manufacturer's protocol. HTRF signals were detected using the EnVision multimode plate reader (PerkinElmer). For the desensitization assay, CHO cells expressing high levels of human FFAR1 (clone 104) were pretreated with the compounds in culture medium for 4 h at 37°C. To remove excess compound, the cells were washed twice with DPBS and treated with compounds in stimulation buffer containing 0.1% fatty acid-free BSA for 30 min at 37°C. Raw data or corrected data were analyzed using Prism 7 (GraphPad Software), and a four-parameter logistic fit equation was used to determine EC_{50} and half-maximal degradation concentration (DC_{50}) for the desensitization analysis.

cAMP HTRF assay for Gαs signaling

Stable human GLP1R-expressing CHO-K1 cells were generated by transfection of pRP[Exp]-Neo-CMV>hGLP1R (VectorBuilder Inc., Chicago, IL, USA) and selection of G418 (0.5 mg/ml; Thermo Fisher Scientific). Stable human GLP1R-expressing CHO-K1 cells and CHO cells expressing high levels of human FFAR1 (clone 104, mycoplasma tested) were plated at a density of 30,000 cells in poly D-lysine-coated 96-well plates, and incubated overnight at 37°C under 5%

CO2. The culture medium was replaced with assay buffer (Hank's balanced salt solution [HBSS] containing 10 mM HEPES [pH 7.5], 0.1% fatty acid-free BSA, and 0.5 mM 3-isobutyl-1-methylxanthine [IBMX]). The cells were then stimulated with drugs for 30 min at 37°C. For the GLP1R desensitization assay, the cells were pretreated with the compounds in Ham's F-12 (FUJIFILM Wako) supplemented with 10% FBS (Thermo Fisher Scientific) at 37°C for 4 h. To remove excess compound, the cells were washed twice with DPBS and treated with compounds at 37°C for 30 min. Intracellular cAMP level was determined using the HTRF cAMP Gs Dynamic Kit (PerkinElmer) according to the manufacturer's instructions. HTRF signals were detected using EnVision. Raw data or corrected data were analyzed using Prism 7, and a four-parameter logistic fit equation was used to determine EC_{50} and DC_{50} for the desensitization analysis.

Serum response factor response element reporter gene assay for Gα12/13 signaling

CHO cells expressing high levels of human FFAR1 (clone 104) were transfected with pGL4.34 (Promega), which contains a luciferase gene with SRF-RE in response to serum response factor through the Gα12/13-RhoA-mediated pathway, using Lipofectamine 3000 (Thermo Fisher Scientific). The transfected cells were plated at 15,000 cells per well in poly D-lysine-coated 384-well white plates. After culturing for 4 h, the culture medium was replaced with assay medium (MEM-α containing 10 mM HEPES (pH 7.5) and 2% FBS) before overnight incubation at 37°C in the presence of 5% CO2. The cells were stimulated with the drugs in the assay medium for 6 h at 37°C, and luciferase activity was measured using EnVision (PerkinElmer) with the Steady-Glo luciferase assay system (Promega). Raw data were analyzed using Prism 7, and a four-parameter logistic fit equation was used to determine EC_{50}.

β-Arrestin recruitment assay

The PathHunter β-arrestin assay (DiscoverX, Fremont, CA, USA) was used to assess β-arrestin recruitment activity. PathHunter® HEK293 cells stably expressing human GPR40, obtained from Takeda Pharmaceutical Company Limited (Tokyo, Japan; mycoplasma tested), were added into poly D-lysine-coated 384-well white plates at 10,000 cells per well in Dulbecco's modified Eagle medium (DMEM) supplemented with 10% dialyzed FBS, 0.05 mg/ml hygromycin B (FUJIFILM Wako), 0.25 mg/ml G418 (FUJIFILM Wako), and 100 U/ml penicillin–streptomycin. After overnight incubation at 37°C in the presence of 5% CO2, the medium was replaced with Opti-MEM® I (Thermo Fisher Scientific) containing 0.1% fatty acid-free BSA. Thereafter, compound stimulation was performed for 4 h at 37°C, followed by incubation with the PathHunter Detection Reagent Solution at 22°C–26°C for 1 h. Luminescence was measured using EnVision. Raw data were analyzed using Prism 7, and a four-parameter logistic fit equation was used to determine EC_{50}.

Animals

Male N-STZ diabetic rats were developed by subcutaneous administration of 120 mg/kg streptozotocin (STZ) to Wistar Kyoto rats (RABICS, LTD., Kanagawa, Japan) at 1.5 days after birth. Saline-injected rats were used as normal control rats. N-STZ rats have been reported to show dysfunction of insulin secretion and action, which is similar to the pathology of human T2DM [82]. All animals were housed in rooms under a 12-h light/dark cycle (light on 0700 h) and had ad libitum access to standard laboratory chow diet (CE-2; CLEA Japan, Inc., Tokyo, Japan) and tap water. The care of the animals and use of the experimental protocols were approved by the Institutional Animal Care and Use Committee of Shonan Health Innovation Park accredited by the American Association for Accreditation of Laboratory Animal Care. For animal experiments, 0.5% methylcellulose was used as the vehicle. All blood samples used in the present study were obtained via the tail vein of the animals.

Sub-chronic study of SCO-267 for evaluating insulin and glucose tolerance

Twenty-five-week-old N-STZ rats were randomized into groups based on body weight, fasting glucose level, and glycosylated hemoglobin (n = 6). The animals were orally administered either SCO-267 (1 and 10 mg/kg) or vehicle once a day for 15 days, followed by a wash-out period of 3 days. The first day of treatment was designated as day 1. ITT and OGTT were performed on day 18 after overnight fasting (17 h). In the ITT, insulin (0.25 IU/kg; Novo-Nordisk, Bagsvaerd, Denmark) was injected subcutaneously, and plasma glucose level was determined at the indicated time points. In the OGTT, glucose (1.5 g/kg) was orally administered, and blood glucose and insulin levels were determined at the indicated time points. The plasma level of SCO-267 was determined before administering glucose in the OGTT.

Chronic study of SCO-267 for evaluating glucose tolerance

Twenty-five-week-old N-STZ rats were fasted for 18 h. The rats were then randomized into groups (n = 6) based on body weight, fasting glucose levels, and glycosylated hemoglobin. The average body weight of N-STZ rats and normal rats was 379 ± 7 and 442 ± 16 g, respectively. The rats were then orally administered test materials (SCO-267, 1 and 10 mg/kg; glibenclamide, 10 mg/kg) or vehicle 60 min before oral glucose loading (1.5 g/kg). The first treatment day was designated as day 1. Glibenclamide, a sulfonylurea that stimulates insulin secretion [83], was used as a reference drug. Thereafter, SCO-267, glibenclamide, or vehicle was repeatedly administered once daily. After the 32nd dose, the rats were fasted for 18 h. Glucose (1.5 g/kg) was orally administered 1 h after the 33rd dose of each material, and plasma parameters were determined at the indicated time points (day 33). A pharmacokinetic study with 1 and 10 mg/kg SCO-267 was conducted under the same experimental conditions (n = 3; after the 33rd dosing). After the drug

wash-out period (days 38–42), the rats were fasted for 16 h (day 43), and the entire pancreas was isolated and homogenized in 75% (v/v) ethanol containing 0.15 M HCl. The homogenized tissues were centrifuged at 8200 × g for 5 min at 4°C. The supernatants were then diluted with phosphate-buffered saline containing 0.1% BSA, and the total insulin level in the supernatants was determined.

Measurement of *in vivo* parameters

Plasma glucose level was measured using an Accu-Chek ST glucometer (Roche Diagnostics, Manheim, Germany) or a 7180 Clinical Analyzer (Hitachi, Tokyo, Japan). Glycosylated hemoglobin was determined using the HLC-723 G8 automated glycosylated hemoglobin analyzer (Tosoh, Tokyo, Japan). Insulin level was determined using an insulin ELISA kit (Cat. No. M1101; Morinaga Institute of Biological Science, Inc., Yokohama, Japan).

Statistical analysis

The experiments performed in this study were exploratory in nature and designed to evaluate the profiles of SCO-267. The current study did not employ a predefined study design; as such, reported P values are descriptive. Statistical significance was analyzed using Bartlett's test for homogeneity of variances, followed by Williams' test ($P > 0.05$) and Shirley-Williams test ($P \leq 0.05$) for evaluating the dose-dependent effects of SCO-267. Alternatively, statistical significance was analyzed using the F test for homogeneity of variances, followed by Student's t-test ($P > 0.2$), or Aspin–Welch test ($P \leq 0.2$) for evaluating the effect of glibenclamide. All tests were conducted using a two-tailed significance level of 5% (0.05). All data are presented as mean ± standard deviation (S.D.).

Results

SCO-267 is a full agonist for GPR40 activating the Gαq, Gαs, and Gα12/13 pathways and β-arrestin recruitment

To determine the potential signaling pathways of SCO-267, I conducted the cell-based IP1 HTRF (for Gαq), cAMP HTRF (for Gαs), SRF-RE reporter gene (for Gα12/13), and β-arrestin recruitment assays (Fig. 15, Table 3). In these assays, AM-1638, fasiglifam, and γ-linolenic acid were used as a representative full allosteric agonist, partial agonist, and endogenous ligand, respectively. In the Gαq-mediated IP1 accumulation assay, SCO-267, AM-1638, fasiglifam, and γ-linolenic acid elevated the IP-1 level in cells expressing high levels of human FFAR1 (Fig. 15A). GPR40 full agonists can activate Gαq signaling even in cells expressing low levels of GPR40 [84]. As shown in Fig. 15B, SCO-267 and AM-1638 were effective (EC_{50} = 0.91, 26 nM, respectively) with similar Emax in CHO cells expressing low levels of human FFAR1, whereas

fasiglifam and γ-linolenic acid were very weak (EC_{50} > 10 and 150 μM, respectively). These data confirmed that SCO-267 is a full agonist, which is consistent with the findings of a previous study [85]. In terms of other signals, SCO-267 and AM-1638 showed potent activity in all assays (Fig. 15C-E), suggesting that these compounds potentiate the Gαq, Gαs, Gα12/13 pathways and β-arrestin recruitment. In addition, the EC_{50} value of SCO-267 was over 10 times lower than that of AM-1638 in all assays.

SCO-267 is allosteric with fasiglifam and an endogenous ligand

GPR40 has three known binding sites: one is an endogenous fatty acid-binding site, the second is where partial agonists such as fasiglifam bind, and the third is where full agonists such as AM-1638 and AP8 bind [65, 68, 70, 72, 86]. As shown in Fig. 15B, SCO-267, fasiglifam, and γ-linolenic acid effectively elevated the IP1 level in CHO cells expressing GPR40. To clarify the binding site of SCO-267, I conducted a titration study of two compounds in a two-dimensional matrix format (Fig. 16). For this matrix analysis, the IP1 HTRF assay was selected because it was identified as the most robust and accurate method compared with the evaluation of other signals (e.g., cAMP and β-arrestin). The presence of fasiglifam (Fig. 16A) or γ-linolenic acid (Fig. 16B) significantly shifted the dose response curve of SCO-267 toward a lower concentration (from 4.6 nM [95% CI, 3.6–6.0 nM] to 0.44 nM [95% CI, 0.31–0.62 nM], or 5.0 nM [95% CI, 3.5–6.9 nM] to 1.7 nM [95% CI, 1.0–2.7 nM] of EC_{50}, respectively). These results indicated that SCO-267 binds at a site different from those for fasiglifam and γ-linolenic acid, and induces positive cooperative effects with these compounds.

SCO-267 activates downstream signaling after chronic exposure in cells

To assess the functional desensitization of GPR40 by SCO-267, I examined the effect of pretreatment with SCO-267 on reactivation of the receptor in the IP1 assay. Chronic exposure to SCO-267 at 37°C for 4 h at less than 10 nM concentration did not cause signal loss compared with the re-stimulation response in the control (Fig. 17A). When the cells were pretreated with 1 μM SCO-267, the re-stimulation response remained at approximately 70%. The desensitization potency of SCO-267 (DC_{50} = 45 nM) was approximately 300 times higher than its EC_{50}. To compare the rate of desensitization to GLP-1 agonism, which has been demonstrated to be effective in clinical settings when chronically exposed [87], I examined the effect of extendin-4 on the re-stimulation of the GLP-1 receptor using the cAMP assay. When the cells were pretreated with 100 nM extendin-4, the re-stimulation response remained at approximately 70% (Fig. 17B). The desensitization potency of extendin-4 (DC_{50} = 100 pM) was approximately four times higher than its EC_{50}. In contrast, the residual response to chronic exposure to fasiglifam, which showed durable efficacy in a 52-week clinical study [64], at 30 μM was approximately 30% (Fig. 17C).

SCO-267 improves insulin sensitivity in N-STZ rats

To explore the effect of chronic exposure to SCO-267 on glucose tolerance and insulin sensitivity, SCO-267 was administered to diabetic N-STZ rats for 15 days and the glucose tolerance and insulin sensitivity were evaluated after the drug wash-out period (Fig. 18). The plasma level of SCO-267 (1 and 10 mg) in rats after the drug wash-out period (day 18) was 0.22 and 0.35 ng/ml, respectively. The unbound SCO-267 concentration calculated using the rat plasma protein binding activity [85] was 1.4 (1 mg/kg SCO-267) and 2.3 pM (10 mg/kg SCO-267), both of which are unlikely to activate GPR40. In fact, the insulin level was not increased in N-STZ rats sub-chronically treated with SCO-267 upon glucose loading (Fig. 18A), and this confirmed the complete removal of SCO-267. In contrast, N-STZ rats sub-chronically treated with SCO-267 (10 mg/kg) showed improved glucose tolerance (Fig. 18B). In addition, the ITT revealed that N-STZ rats sub-chronically treated with SCO-267 (10 mg/kg) showed increased insulin sensitivity (Fig. 18C).

SCO-267 exerts sustained glucose-lowering effect after administration in N-STZ rats

To explore whether chronic exposure to SCO-267 is effective in improving glycemic control *in vivo*, I evaluated glucose tolerance after the first and repeated dosing of SCO-267 (1 and 10 mg/kg) in N-STZ rats. In this experiment, food intake levels were lower and body weight was decreased in the 10 mg/kg SCO-267 dose group (Fig. 19A and 19B). In the OGTT, after the first dose, SCO-267 significantly increased insulin secretion and improved glucose tolerance, which were superior to those in normal rats (Fig. 19C and 19D). As shown in Fig. 19E, the plasma level of SCO-267 was 28.8 ± 1.5 and 24.2 ± 2.3 ng/ml before the 33rd dose of 10 mg/kg SCO-267 (time = 0) and after 24 h. In the OGTT after the 33rd dosing (day 33), SCO-267 still increased insulin secretion and improved glucose tolerance, which were superior to those in normal rats (Fig. 19F and 19G). Glibenclamide showed a trend of improvement in glucose tolerance after the first dose, and impaired glucose tolerance after the 33rd dose (Fig. 19C, 19D, 19F, and 19G). In addition to the sustained glucose-lowering effect, SCO-267 increased pancreatic insulin level at the end of the study (Fig. 19H).

Discussion

In this study, I revealed that SCO-267, a GPR40 full allosteric agonist, was still effective in activating downstream signaling after chronic exposure *in vitro* and *in vivo*. The *in vitro* experiments showed that SCO-267 activated the Gαq, Gαs, Gα12/13 pathways, and β-arrestin recruitment, and bound to a site different from that of fasiglifam and the endogenous ligand with

positive cooperativity. The *in vitro* desensitization analysis using GPR40-overexpressing cells showed that GPR40 could be re-activated by SCO-267 after 4 h of exposure to SCO-267. By using N-STZ rats, I showed that SCO-267 treatment for 15 days improved glucose tolerance by increasing insulin sensitivity. A 33-day repeated dose study, in which GPR40 was constantly exposed to SCO-267, revealed that repeated dosing with SCO-267 was effective in inducing a durable therapeutic efficacy in lowering glucose level and increasing insulin level in N-STZ rats.

In the IP1 accumulation assay, the Emax of SCO-267 was as high as that of AM-1638, a well-studied GPR40 full agonist, in CHO cells expressing low levels of human FFAR1, indicating that SCO-267 is a GPR40 full agonist. In addition, SCO-267 showed positive cooperativity with fasiglifam or γ-linolenic acid in the IP1 accumulation assay, indicating that SCO-267 is allosteric with either fasiglifam or the endogenous ligand. These results demonstrated that SCO-267 is an allosteric full agonist of GPR40.

SCO-267 was efficacious in activating downstream signaling even after chronic exposure in human GPR40-expressing CHO cells, similar to exendin-4. Pretreatment of cells with SCO-267 for 4 h at high concentrations (≥100 nM) caused only 30% loss of re-stimulation response, similar to that of exendin-4. The loss rate of the re-stimulation response was higher with fasiglifam, which showed a 70% loss of re-stimulation response. These findings indicate that SCO-267-mediated chronic activation of GPR40 may not be efficacious in desensitizing downstream signaling, which is likely an important characteristic of an agonistic drug candidate.

In the chronic dose study in rats, the plasma SCO-267 concentration immediately before and 24 h after the 33rd dose of 10 mg/kg SCO-267 was 28.8 and 24.2 ng/ml, respectively. In a previous study, N-STZ rats dosed with SCO-267 (0.3 mg/kg, Cmax = 22.7 ng/ml) potently stimulated insulin secretion and improved glucose tolerance [85]. This suggests that the plasma level of exposure achieved by 10 mg/kg SCO-267 was high enough to activate GPR40 throughout the day in our chronic dosing study in N-STZ rats. Even under these conditions, the sustained efficacy of SCO-267 on the glucose-lowering effect, which was superior to that in normal rats, was observed upon drug dosing. The continuous glucose-lowering effect of exendin-4 was confirmed in patients with T2DM after 30 weeks of treatment [88]. In addition, the effect of fasiglifam has been confirmed in rats treated for 6 weeks [89] and in patients with T2DM after 52 weeks of treatment [64]. Taken together with the present *in vitro* observations, in which SCO-267 showed equal or less desensitization to exendin-4 and fasiglifam, SCO-267 may induce similar durability of therapeutic efficacy in patients.

Notably, after the drug wash-out period, N-STZ rats treated with SCO-267 for 15 days showed increased insulin sensitivity. In this study, food intake and body weight were lowered in SCO-267-treated N-STZ rats. Hence, increased insulin sensitivity may be the indirect result of weight loss. Moreover, GLP-1 stimulation by SCO-267 may have contributed to the increased insulin

sensitivity. Our previous data showed that SCO-267 stimulated GLP-1 in N-STZ rats [85]. GLP-1 is known to promote peripheral glucose uptake and reduce hepatic glucose production partially through the central nervous system [90]. Further studies are required to investigate the mechanism of SCO-267 dosing on increased insulin sensitivity.

STZ treatment causes abnormalities in insulin secretion and β-cell function [91]. Interestingly, chronic exposure of N-STZ rats to SCO-267 significantly increased the pancreatic insulin level. Considering that hyperglycemia induces glucotoxicity, which results in β-cell dysfunction [92], the increase may have been caused by a decrease in glucotoxicity via the glucose-lowering activity of SCO-267. Furthermore, it has been reported that vincamine, a monoterpenoid indole alkaloid, which activates GPR40, protected STZ-treated INS-832/13 cells, a rat insulinoma cell line, through GPR40 activation [93], and CNX-011-67, a GPR40 agonist, reduces inflammation-induced apoptosis of NIT1 cells, a mouse pancreatic β-cell line [94]. Overall, SCO-267 may improve β-cell function through a direct GPR40-mediated effect.

In summary, I revealed that even after chronic exposure, SCO-267 effectively activates GPR40 in cells and rats. In diabetic rats, chronic exposure to SCO-267 was highly effective in improving glucose tolerance. My findings suggest that sustained exposure to SCO-267 likely induces a durable glucose-lowering effect without tachyphylaxis in patients with diabetes.

Figures and Tables

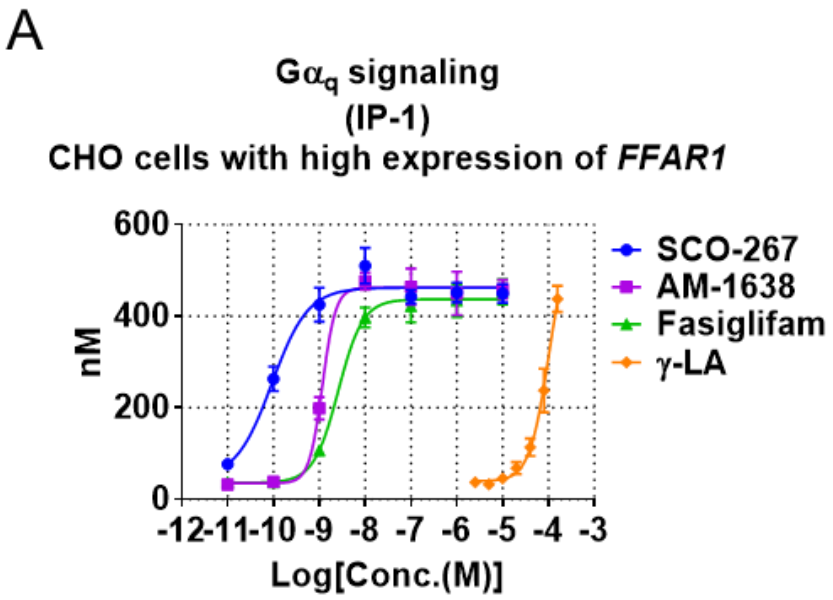

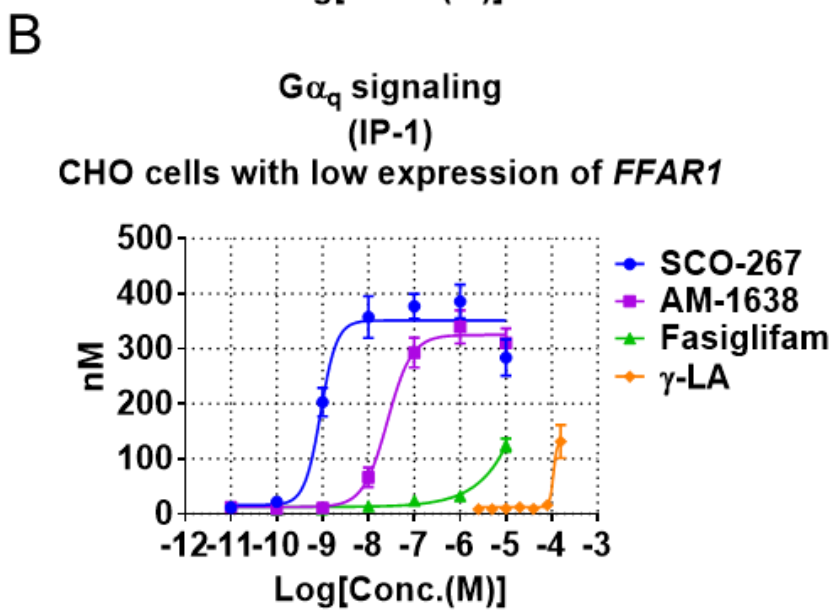

C

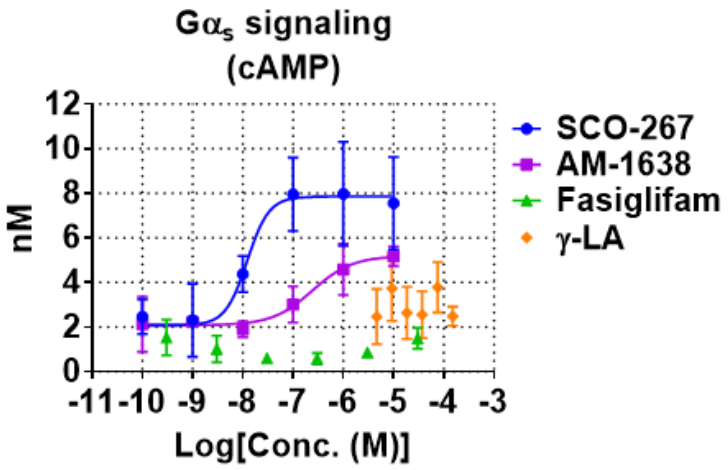
Gαs signaling
(cAMP)
nM
12
10
8
6
4
2
0
-11 -10 -9 -8 -7 -6 -5 -4 -3
Log[Conc. (M)]
SCO-267
AM-1638
Fasiglifam
γ-LA

D

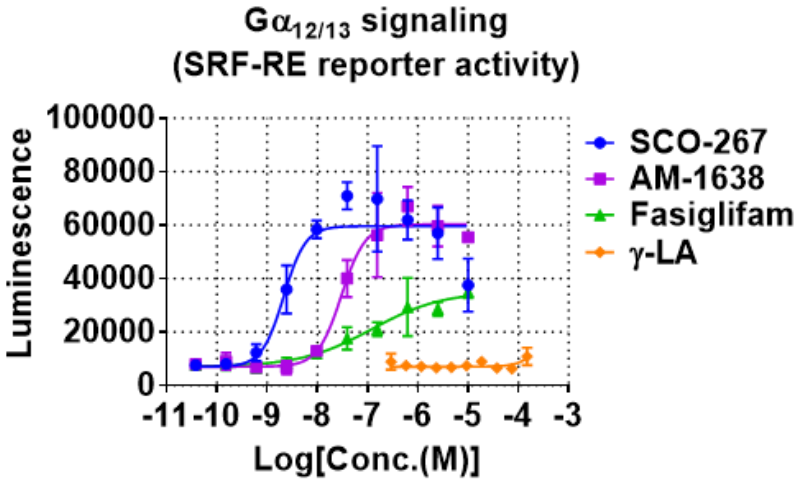
Gα12/13 signaling
(SRF-RE reporter activity)
Luminescence
100000
80000
60000
40000
20000
0
-11 -10 -9 -8 -7 -6 -5 -4 -3
Log[Conc.(M)]
SCO-267
AM-1638
Fasiglifam
γ-LA

E

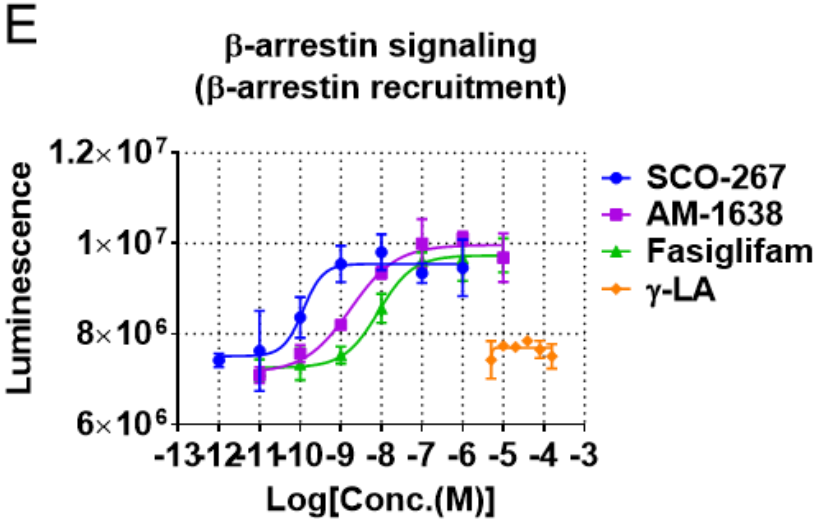
β-arrestin signaling
(β-arrestin recruitment)
Luminescence
1.2×10^7
1×10^7
8×10^6
6×10^6
-13 -12 -11 -10 -9 -8 -7 -6 -5 -4 -3
Log[Conc.(M)]
SCO-267
AM-1638
Fasiglifam
γ-LA

Figure 15. Effects of SCO-267 on the Gαq, Gαs, and Gα12/13 signals, and β-arrestin recruitment. The effects of SCO-267, AM-1638, fasiglifam, and γ-linolenic acid were analyzed by myo-inositol 1 phosphate (IP1) accumulation in CHO cells expressing high (A) and low (B) levels of human FFAR1, cAMP production (C), SRF-RE response (D), and β-arrestin recruitment (E). Representative graphs from two (for C, D, and E) or three (for A and B) independent experiments are shown. The data are presented as mean ± S.D. of four technical replicates (A, B, E), three technical replicates, except SCO-267, with five technical replicates (C), and three technical replicates (D). γ-LA, γ-linolenic acid.

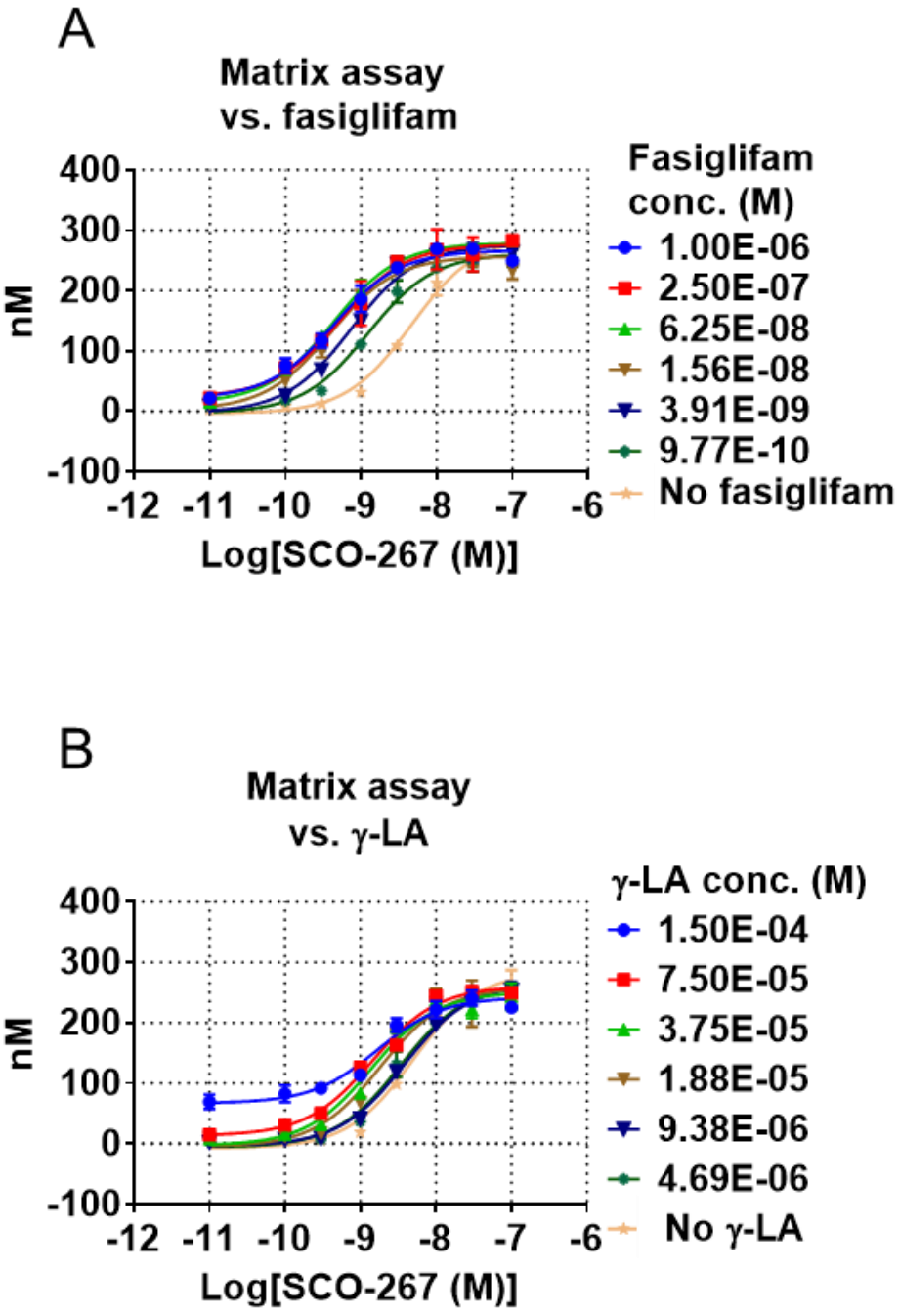

Figure 16. Effects of increasing concentrations of fasiglifam or γ-linolenic acid on the dose–response curve of SCO-267. The IP1 accumulation assay of SCO-267 in the presence of fasiglifam (A) or γ-linolenic acid (B) at various concentrations using CHO cells expressing low levels of human FFAR1 (clone 2). Representative graphs of two independent experiments are shown. The data are presented as mean ± S.D. of two technical replicates. γ-LA, γ-linolenic acid.

A

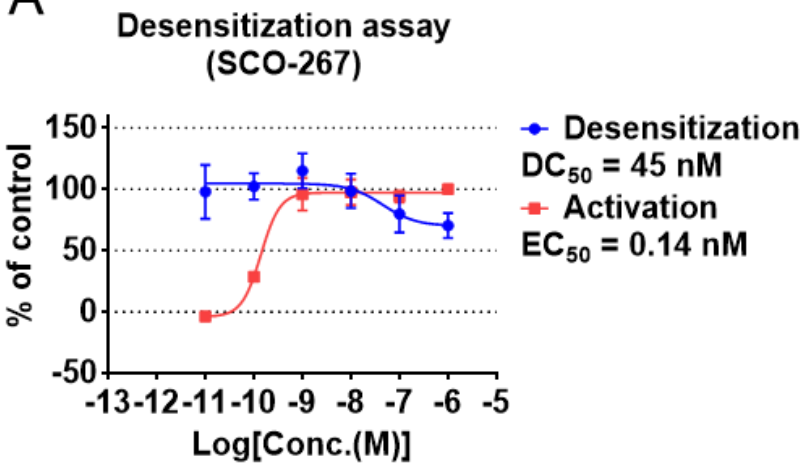
Desensitization assay
(SCO-267)
% of control
150
100
50
0
-50
-13 -12 -11 -10 -9 -8 -7 -6 -5
Log[Conc.(M)]
Desensitization
DC50 = 45 nM
Activation
EC50 = 0.14 nM

B

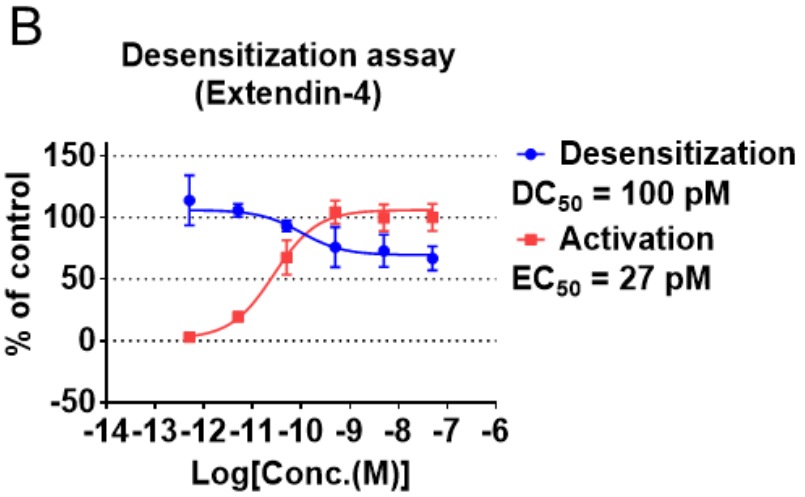
Desensitization assay
(Extendin-4)
% of control
150
100
50
0
-50
-14 -13 -12 -11 -10 -9 -8 -7 -6
Log[Conc.(M)]
Desensitization
DC50 = 100 pM
Activation
EC50 = 27 pM

C

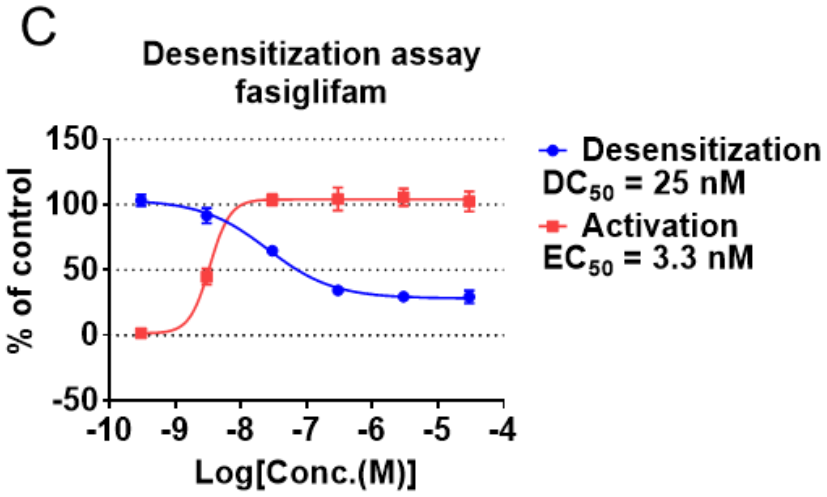
Desensitization assay
fasiglifam
% of control
150
100
50
0
-50
-10 -9 -8 -7 -6 -5 -4
Log[Conc.(M)]
Desensitization
DC50 = 25 nM
Activation
EC50 = 3.3 nM

Figure 17. Prolonged stimulation effect of SCO-267 in the IP1 accumulation assay. (A) CHO cells stably expressing high levels of human FFAR1 (clone 104) were pretreated with the indicated concentrations of SCO-267 for 4 h at 37°C before excess ligand was removed by washing. The cells were then re-stimulated with 300 nM SCO-267 for 30 min at 37°C, and the IP1 level was measured (● Desensitization). At the same time, the cells were also stimulated with various concentrations of SCO-267 after DMSO pretreatment (■ Activation). IP1 response is expressed as a percent of control, in which the cells treated with 1000 nM SCO-267 for 30 min after dimethyl sulfoxide (DMSO) pretreatment were used as 100% controls [95] and the cells treated with DMSO for 30 min after DMSO pretreatment were used as 0% controls (bottom). (B) CHO-cells stably expressing human GLP1R were pretreated with the indicated concentrations of extendin-4 for 4 h at 37°C before excess ligand was removed by washing. The cells were re-stimulated with 10 nM extendin-4 for 30 min at 37°C, and the intracellular cAMP level was measured (● Desensitization). At the same time, the cells were also stimulated with extendin-4 at various concentrations after DMSO pretreatment (■ Activation). cAMP response was expressed as a percent of control, in which the cells treated with 10 nM extendin-4 for 30 min after DMSO pretreatment were used as 100% controls [95] and the cells treated with DMSO for 30 min after DMSO pretreatment were used as 0% controls (bottom). Representative graphs of two independent experiments are shown. The data are presented as mean ± S.D. of three technical replicates. DC_{50}, the half-maximal desensitization concentration.

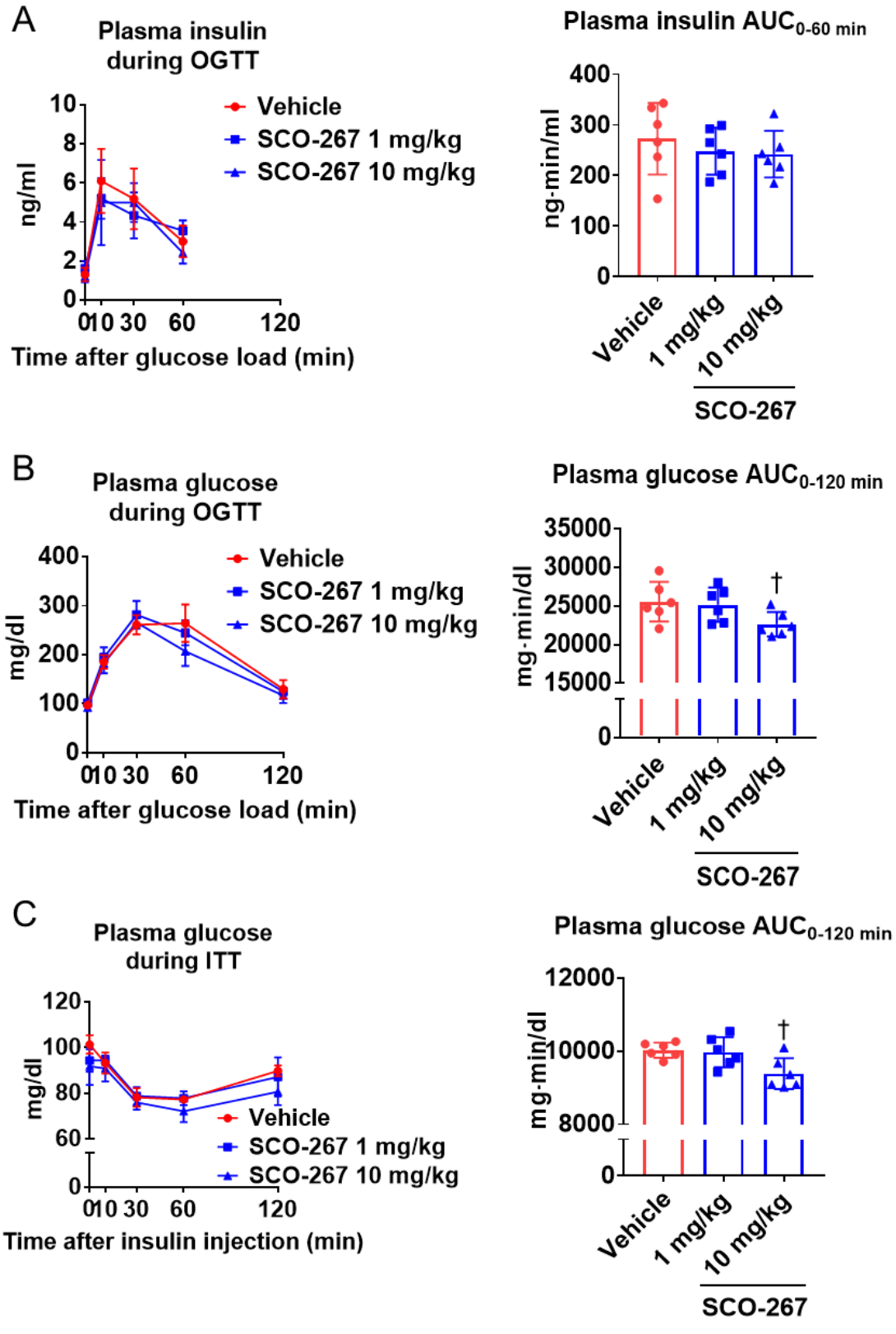
A
Plasma insulin during OGTT
ng/ml
Vehicle
SCO-267 1 mg/kg
SCO-267 10 mg/kg
Time after glucose load (min)
Plasma insulin AUC0-60 min
ng·min/ml
Vehicle
1 mg/kg
10 mg/kg
SCO-267
B
Plasma glucose during OGTT
mg/dl
Vehicle
SCO-267 1 mg/kg
SCO-267 10 mg/kg
Time after glucose load (min)
Plasma glucose AUC0-120 min
mg·min/dl
†
Vehicle
1 mg/kg
10 mg/kg
SCO-267
C
Plasma glucose during ITT
mg/dl
Vehicle
SCO-267 1 mg/kg
SCO-267 10 mg/kg
Time after insulin injection (min)
Plasma glucose AUC0-120 min
mg·min/dl
†
Vehicle
1 mg/kg
10 mg/kg
SCO-267

Figure 18. Effect of sub-chronic administration of SCO-267 on glucose tolerance and insulin sensitivity in N-STZ rats. Vehicle or SCO-267 (1 or 10 mg/kg) was orally administered once a day for 15 days following a drug wash-out period of 3 days. (A) Plasma insulin level and AUC during the OGTT. (B) Plasma glucose level and AUC during the OGTT. (C) Plasma glucose level and AUC during the ITT. †$P < 0.05$ vs. vehicle by Williams' test. Values are presented as mean ± S.D. (n = 6, biological replicates).

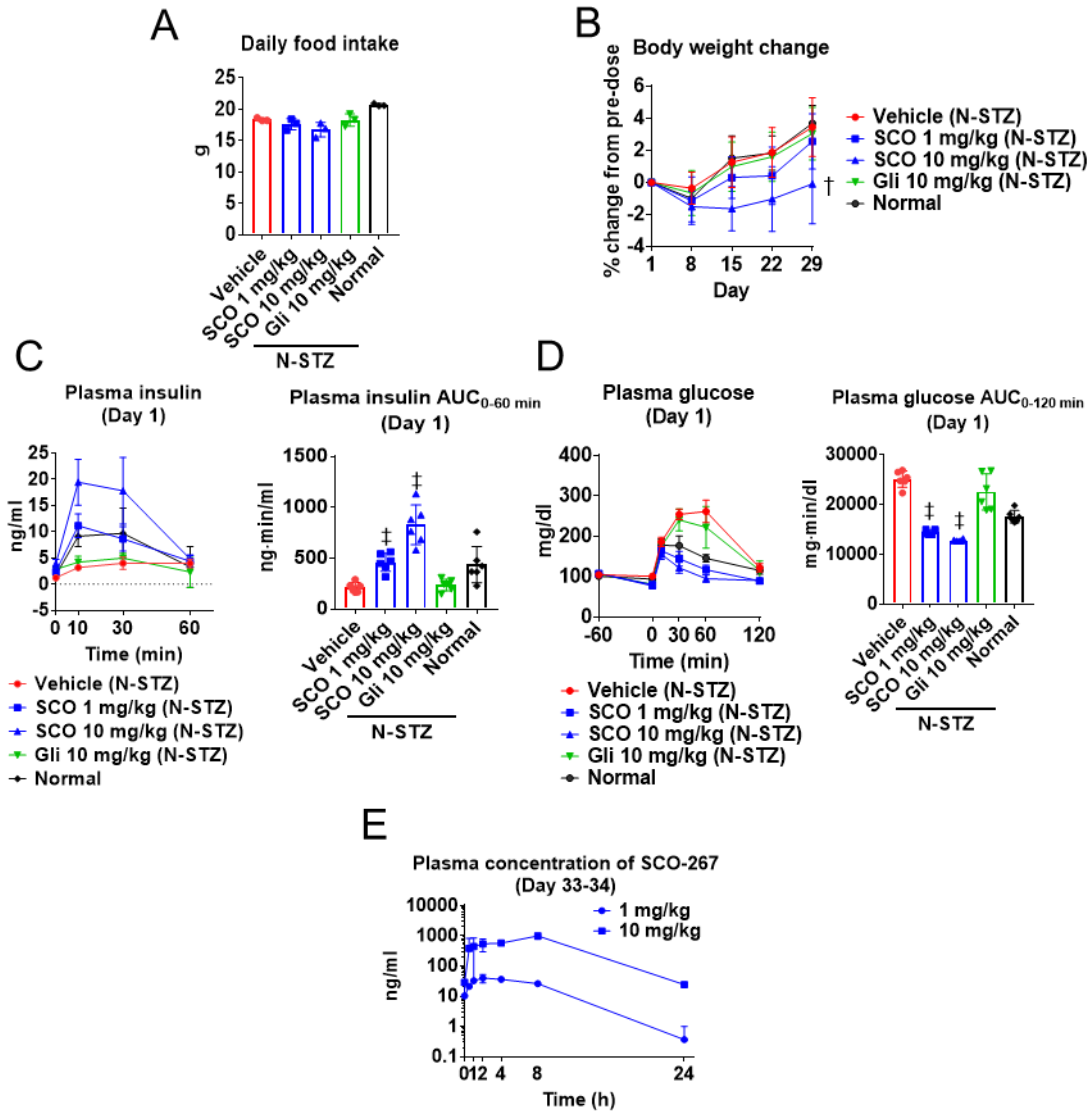
A
Daily food intake
g
Vehicle
SCO 1 mg/kg
SCO 10 mg/kg
Gli 10 mg/kg
Normal
N-STZ
B
Body weight change
% change from pre-dose
Day
Vehicle (N-STZ)
SCO 1 mg/kg (N-STZ)
SCO 10 mg/kg (N-STZ)
Gli 10 mg/kg (N-STZ)
Normal
C
Plasma insulin (Day 1)
ng/ml
Time (min)
Plasma insulin AUC0-60 min (Day 1)
ng·min/ml
D
Plasma glucose (Day 1)
mg/dl
Time (min)
Plasma glucose AUC0-120 min (Day 1)
mg·min/dl
E
Plasma concentration of SCO-267 (Day 33-34)
ng/ml
Time (h)
1 mg/kg
10 mg/kg

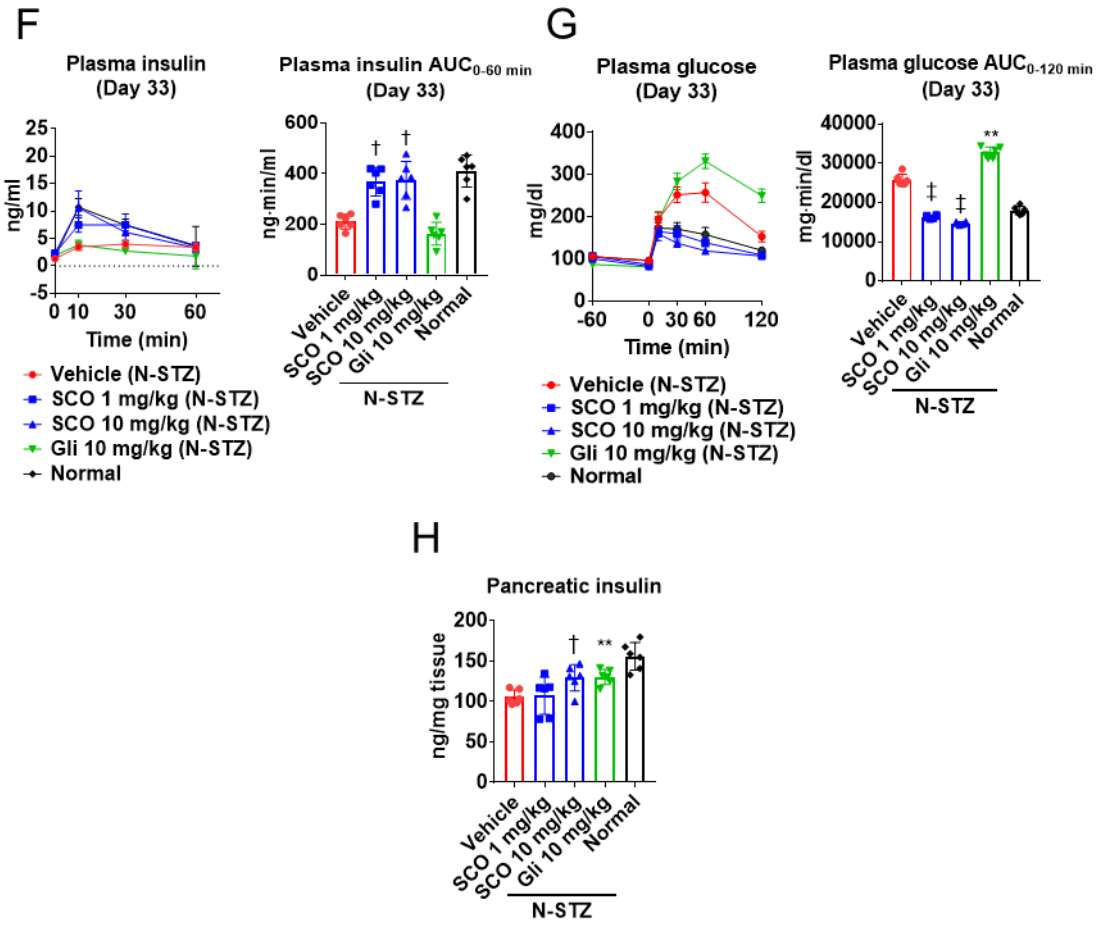

Figure 19. Effect of chronic administration of SCO-267 in N-STZ rats. Vehicle, SCO-267 (1 or 10 mg/kg), or glibenclamide (10 mg/kg) was repeatedly administered to N-STZ rats. (A) Daily food intake. (B) Body weight change (the average baseline body weight of N-STZ rats and normal rats was 379 ± 7 g and 442 ± 16 g, respectively.). Plasma insulin level (C) and plasma glucose level (D) during the OGTT on day 1. (E) Pharmacokinetics analysis of SCO-267 in N-STZ rats on days 33 and 34. Plasma insulin level (F) and plasma glucose level (G) during the OGTT on day 33. Pancreatic insulin level on day 43 (H). †$P < 0.05$ and ‡$P < 0.05$ vs. vehicle by Williams' test and Shirley–Williams test, respectively. **$P < 0.01$ vs. vehicle by Student's t-test. Values are presented as mean ± S.D. (n = 6 for chronic dose study except n = 3 for daily food intake and n = 3 for pharmacokinetic study, biological replicates). SCO, SCO-267. Gli, glibenclamide.

Table 3. Pharmacological potencies of SCO-267

Test Material	$G\alpha_q$ (IP1) high *FFAR1* expression	$G\alpha_q$ (IP1) low *FFAR1* expression	$G\alpha_s$ (cAMP)	$G\alpha_{12/13}$ (SRF-RE reporter activity)	β-Arrestin (β-arrestin recruitment)
			EC_{50} [95% CI] nM		
SCO-267	0.093 [0.035–0.14]	0.91 [0.52–1.2]	12 [5.8–30]	2.1 [1.1–3.7]	0.12 [0.032–0.31]
AM-1638	1.2 [1.1–1.5]	26 [19–35]	240 [65–8900]	30 [22–42]	1.7 [0.61–3.8]
Fasiglifam	2.6 [1.9–3.4]	>10,000	>30,000	120 [42–1500]	8.5 [4.4–15]
γ-LA	N.A.	>150,000	>150,000	>150,000	>150,000

Data are representative of two experiments performed in three or four technical replicates. γ-LA, γ-linolenic acid; CI, confidence interval; N.A., not applicable.

General Discussion

In the first part of study, I clarified that cholesterol buried in RORγt protein impedes the potency of RORγt inverse agonist by *in vitro* experiments. Furthermore, through HTS with the protein without cholesterol, I successfully identified a novel cholesterol-competitive RORγt inverse agonist, which was origin of TAK-828F effective in murine colitis model [45] and murine experimental autoimmune encephalomyelitis (EAE) model [96].

This study showed that the inhibitory effect of cholesterol on the potency of RORγt inverse agonist was observed even in cell-based assay, in which IC_{50} of Compound 1 with normal medium and cholesterol-depleted medium were 14 μM and 3.1 μM respectively. Although TAK-828F had sufficient potency to show efficacy in the murine model, our results will bring forward an approach to develop ligand independent molecules, such as allosteric modulator. In fact, MRL-871, which binds to the sites different from orthosteric cholesterol binding site, showed inhibition of cofactor binding independent of cholesterol concentration [97]. Furthermore, compound 3, another RORγt allosteric inhibitor, reduced Th17-dependent response by 45% with plasma concentration above IC_{50} in imiquimod induced murine skin inflammation model, although VTP-43742, cholesterol-competitive inverse agonist required plasma concentration above IC_{90} achieved the same level of response [98].

Besides Th17 cells, RORγt is expressed in various immune cells such as CD4+CD8+ double positive thymocytes, Tc17, regulatory T cell, innate lymphoid 3 cells, NK cells, and γδ T cells [99]. Although the role of RORγt in the differentiation and function of Th17 cells has been well-studied, the function of the receptor and the effect of RORγt inverse agonists on other RORγt-expressing cells, such as regulatory T cell, NK cells, and γδ T cells, require further investigation. Especially, it was reported that regulatory T cells, known as Tr17 cells, a novel subset of Treg cells, is RORγt+Foxp3+ double positive and plays an important role in the regulation of auto immune arthritis in mice through a specific repression of Th17 cells [100]. These results provide a view of the complex mechanism of RORγt in immune system and inflammation. Recently, it showed that different RORγ antagonists has distinct activity in regulation of RORγ function in a cell- and gene-program specific manner, which is thought to be the result of difference in NR-cofactor- histone modifying enzymes complex and chromatin accessibility [101]. Therefore, various tool compounds should be used for elucidating the role of RORγt in each immune cell types.

RORγt orthosteric inverse agonists including VTP43742 has already demonstrated clinical efficacy with reduction of plasma IL-17 level against psoriasis patients, but recent clinical trials have been terminated due to safety reasons observed in human or preclinical studies [102]. For example, loss of RORγt function leads to apoptosis in CD4+CD8+ double positive thymocytes and reduction of single-positive T lymphocytes [103]. In addition, Thymic Lymphoma was

observed in a 6 months carcinogenicity test with BMS-986251 using rasH2-Tg mice [104]. These results provoked a tissue-specific strategy inhibiting Th17 cells differentiation without reduction of thymocyte maturation and cancer risks. My novel cholesterol-competitive RORγt inverse agonists and TAK-828F may serve as additional tools for clarifying the role of RORγt in each cell and our sensitive HTS will be useful for developing a tissue selective modulator reducing risk of thymoma.

In the second part of study, I revealed that SCO-267 is allosteric full agonist activating Gαs, Gαi, Gαq, Gα12/13, and β-arrestin signals. Furthermore, by using GPR40-expressed cell line and diabetic rat model, I showed that GPR40 stimulated chronically by SCO-267 has durable efficacy in downstream signaling and glucose control. This study will provide a novel treatment strategy for chronic diseases besides diabetes. For example, NAFLD is a range of chronic liver diseases that is characterized by steatosis and absence of alcohol consumption [105]. NAFLD provokes other liver disease and has been rapidly increasing in Western country, but there are no approved drugs. In CDAHFD-fed murine non-diabetic NAFLD model, chronic treatment of SCO-267 for 4 weeks induced glucagon and GLP-1 stimulation, and improved liver condition without glucose lowering or body weight reduction [106]. Stimulation of insulin, glucagon, GLP-1, glucose-dependent insulinotropic polypeptide, and peptide YY was also observed in human clinical trials [107]. Together with these results, this study supports further development of SCO-267 for chronic disease including diabetes, obesity, and NAFLD.

GPCR signaling is regulated by ligand types, the intrinsic properties of the receptor and G proteins, as well as trafficking of the receptor. After agonist stimulation and downstream activation, dissociation of G protein and receptor occur. Then, the agonist-bound receptor is phosphorylated by GRKs, resulted in the β-arrestin recruitment. This interaction inhibits further coupling to the G proteins, hence desensitizing the G-protein mediated response [108].The interaction also leads to formation of a multiprotein complex with clathrin and AP2, to undergo endocytosis [109]. The receptor phosphorylation pattern depends on the cell type and the agonist, resulted in diverse function of efficacy, internalization, and degradation [110, 111]. Recently different agonists were shown to produce different response pattern through coupling of different types of G protein, known as “biased agonism” [112]. This concept provided a mitigation strategy avoiding desensitization. In fact, CCL19, a physiological ligand of CCR7, induced Gαq signal and β-arrestin interaction with desensitization, whereas CCL21, which does not induce β-arrestin recruitment, activated signal response without receptor desensitization [113]. However, I revealed that SCO-267 showed sustained signaling of GPR40 in spite of the ability of β-arrestin recruitment. This unexpected result might be explained by resensitization. β-arrestin plays a pivotal role in not only GPCR desensitization and internalization but also trafficking and resensitization. Generally, Class A GPCRs, including β2AR and GPR40, tend to bind to β-arrestin

with low affinity, then are dissociated from β-arrestin, dephosphorylated, and rapidly recycled back to the plasma membrane. In contrast, Class B GPCRs, such as V2R and PTHR, exhibit stable binding to β-arrestin with high affinity resulting in sustained endocytosis and delayed trafficking to the plasma membrane [22]. Besides β-arrestin, the Rab GTPase, subfamily of the Ras GTPase, is known to play an important role in trafficking of the GPCR [114]. Maturement from early to late endosome or recycling endosome are dictated by the recruitment and presence of Rab subtype (Fig. 20). Rab5 localizes to the plasma membrane, and supports GPCR internalization to early endosome [115]. Rab4 is required for rapid receptor recycling from the early endosome to the plasma membrane, whereas Rab9 is involved in transfer to late endosome. Rab11 aids slow recycling to the plasma membrane, while Rab7 regulates the trafficking to lysosomes for degradation. Recently the application of FRET-based sensor allows real-time observation of signaling and trafficking in live cells [116]. This method revealed that DHA, an endogenous ligand of GPR120 which is a subtype of GPR40, induced fast GPR120-Rab4 interaction within 3 mins indicating rapid recycling to the plasma membrane [117], consistent with the report that internalized GPR40 stimulated by linoleic acid was localized to Rab4/Rab5 positive endosome but not to lysosomes for degradation, and was rapidly recycled back to the plasma membrane [118]. Although further studies are necessary to understand mechanism of Rab protein and GPCR trafficking, I believed that SCO-267, which exhibits sustained effect, is useful chemical tool for these biochemical studies.

In summary, it is important to reveal the mechanism of the target receptors. Through this research, I revealed the relationship between the endogenous ligand and the inverse agonists in RORγt and durability of the full agonist in GPR40. These insight and novel tool compounds may be helpful for further understanding of each receptor biology respectively and may be applicable for drug discovery research targeting other receptors.

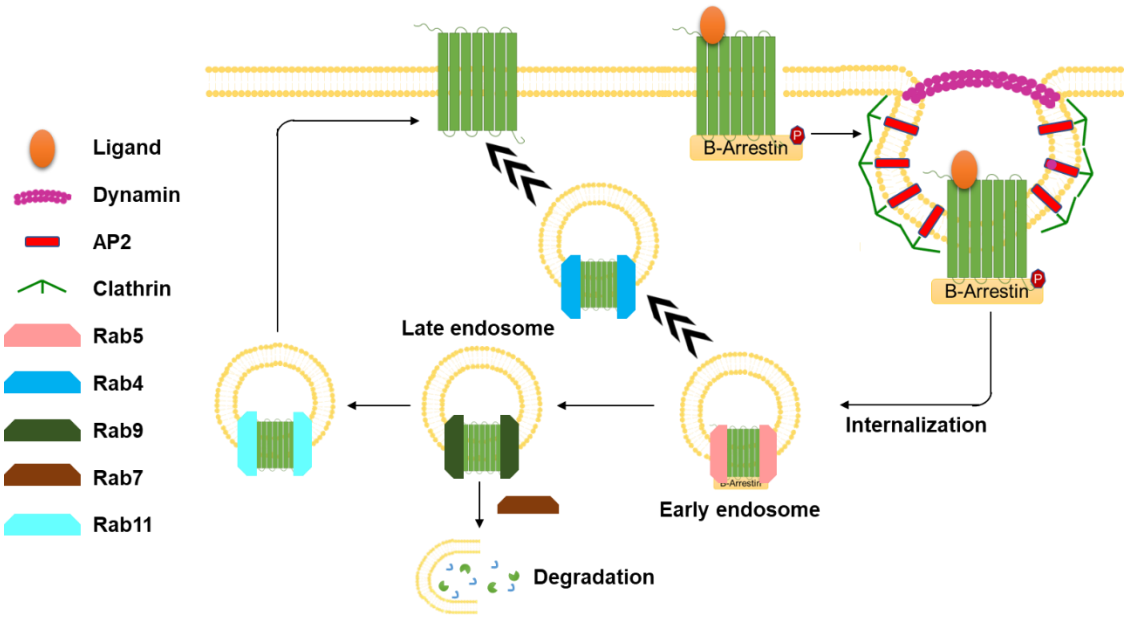

Figure 20. Schematic representation of Rab proteins in GPCR trafficking

Acknowledgements

I really appreciate Professor Kazuich Sakamoto, the University of Tsukuba, guiding my work with valuable discussion throughout my doctoral program.

I greatly thank Dr. Hidehisa Iwata and Dr. Yusuke Moritoh for valuable suggestions, contributions, and helpful supports. I also thank all of the co-authors of the articles incorporated in this dissertation.

I also thank Dr. Manabu Furukawa and Yoshio Iwakawa, Nippon Boehringer Ingelheim Co., Ltd., for their understanding and support on my doctoral program.

Finally, I would like to appreciate my wife and daughters supporting my life at the University of Tsukuba.

References

1. Overington, J.P., B. Al-Lazikani, and A.L. Hopkins, *How many drug targets are there?* Nature Reviews Drug Discovery, 2006. **5**(12): p. 993-996.
2. Christopoulos, A., *Allosteric binding sites on cell-surface receptors: novel targets for drug discovery.* Nature Reviews Drug Discovery, 2002. **1**(3): p. 198-210.
3. Kenakin, T. and L.J. Miller, *Seven transmembrane receptors as shapeshifting proteins: the impact of allosteric modulation and functional selectivity on new drug discovery.* Pharmacol Rev, 2010. **62**(2): p. 265-304.
4. Kininis, M. and W.L. Kraus, *A global view of transcriptional regulation by nuclear receptors: gene expression, factor localization, and DNA sequence analysis.* Nucl Recept Signal, 2008. **6**: p. e005.
5. Gustafsson, J.-A., *Historical overview of nuclear receptors.* The Journal of Steroid Biochemistry and Molecular Biology, 2016. **157**: p. 3-6.
6. Govindan, M.V., *et al*., *Cloning of the human glucocorticoid receptor cDNA.* Nucleic Acids Res, 1985. **13**(23): p. 8293-304.
7. Weikum, E.R., X. Liu, and E.A. Ortlund, *The nuclear receptor superfamily: A structural perspective.* Protein Sci, 2018. **27**(11): p. 1876-1892.
8. Kumar, R. and E.B. Thompson, *Transactivation functions of the N-terminal domains of nuclear hormone receptors: protein folding and coactivator interactions.* Mol Endocrinol, 2003. **17**(1): p. 1-10.
9. Moras, D. and H. Gronemeyer, *The nuclear receptor ligand-binding domain: structure and function.* Curr Opin Cell Biol, 1998. **10**(3): p. 384-91.
10. Acevedo, M.L. and W.L. Kraus, *Transcriptional activation by nuclear receptors.* Essays Biochem, 2004. **40**: p. 73-88.
11. Mazaira, G.I., *et al*., *The Nuclear Receptor Field: A Historical Overview and Future Challenges.* Nucl Receptor Res, 2018. **5**.
12. Mullican, S.E., J.R. Dispirito, and M.A. Lazar, *The orphan nuclear receptors at their 25-year reunion.* J Mol Endocrinol, 2013. **51**(3): p. T115-40.
13. Evans, R.M. and D.J. Mangelsdorf, *Nuclear Receptors, RXR, and the Big Bang.* Cell, 2014. **157**(1): p. 255-66.
14. Nanduri, R., *et al*., *ONRLDB--manually curated database of experimentally validated ligands for orphan nuclear receptors: insights into new drug discovery.* Database (Oxford), 2015.
15. Rajagopal, S., K. Rajagopal, and R.J. Lefkowitz, *Teaching old receptors new tricks: biasing seven-transmembrane receptors.* Nature Reviews Drug Discovery, 2010. **9**(5): p.

373-386.

16. Katritch, V., V. Cherezov, and R.C. Stevens, *Structure-function of the G protein-coupled receptor superfamily.* Annu Rev Pharmacol Toxicol, 2013. **53**: p. 531-56.
17. Yang, D., *et al*., *G protein-coupled receptors: structure- and function-based drug discovery.* Signal Transduct Target Ther, 2021. **6**(1): p. 7.
18. Wettschureck, N. and S. Offermanns, *Mammalian G Proteins and Their Cell Type Specific Functions.* Physiological Reviews, 2005. **85**(4): p. 1159-1204.
19. Pedro, M.P., K. Lund, and R. Iglesias-Bartolome, *The landscape of GPCR signaling in the regulation of epidermal stem cell fate and skin homeostasis.* STEM CELLS, 2020. **38**(12): p. 1520-1531.
20. Siehler, S., *G12/13-dependent signaling of G-protein-coupled receptors: disease context and impact on drug discovery.* Expert Opin Drug Discov, 2007. **2**(12): p. 1591-604.
21. Hilger, D., M. Masureel, and B.K. Kobilka, *Structure and dynamics of GPCR signaling complexes.* Nat Struct Mol Biol, 2018. **25**(1): p. 4-12.
22. Mohan, M.L., *et al*., *G-protein coupled receptor resensitization-appreciating the balancing act of receptor function.* Curr Mol Pharmacol, 2012.
23. Martínez-Morales, J.C., *et al*., *Cell Trafficking and Function of G Protein-coupled Receptors.* Arch Med Res, 2022. **53**(5): p. 451-460.
24. Jetten, A.M., *Retinoid-Related Orphan Receptors (RORs): Critical Roles in Development, Immunity, Circadian Rhythm, and Cellular Metabolism.* Nuclear Receptor Signaling, 2009;7:e003.
25. He, Y.-W., *et al*., *RORgammat, a Novel Isoform of an Orphan Receptor, Negatively Regulates Fas Ligand Expression and IL-2 Production in T Cells.* Immunity, 1998. **9**(6): p. 797-806.
26. Ghoreschi, K., *et al*., *T helper 17 cell heterogeneity and pathogenicity in autoimmune disease.* Trends in Immunology, 2011. **32**(9): p. 395-401.
27. Korn, T., *et al*., *IL-17 and Th17 Cells.* Annual Review of Immunology, 2009. **27**(1): p. 485-517.
28. Littman, D.R. and A.Y. Rudensky, *Th17 and Regulatory T Cells in Mediating and Restraining Inflammation.* Cell, 2010. **140**(6): p. 845-858.
29. Yang, X.O., *et al*., *T Helper 17 Lineage Differentiation Is Programmed by Orphan Nuclear Receptors RORalpha and RORgamma.* Immunity, 2008. **28**(1): p. 29-39.
30. Chang, M.R., H. Rosen, and P.R. Griffin, *RORs in autoimmune disease.* Curr Top Microbiol Immunol, 2014. **378**: p. 171-82.
31. Eberl, G. and D.R. Littman, *The role of the nuclear hormone receptor RORγt in the development of lymph nodes and Peyer's patches.* Immunological Reviews, 2003. **195**(1):

p. 81-90.

32. Țiburcă, L., *et al*., *The Treatment with Interleukin 17 Inhibitors and Immune-Mediated Inflammatory Diseases.* Current Issues in Molecular Biology, 2022. **44**(5): p. 1851-1866.
33. Kumar, N., *et al*., *The Benzenesulfoamide T0901317 Is a Novel Retinoic Acid Receptor-Related Orphan Receptor-α/γ Inverse Agonist.* Molecular Pharmacology, 2010. **77**(2): p. 228-236.
34. Kojetin, D.J. and T.P. Burris, *REV-ERB and ROR nuclear receptors as drug targets.* Nature Reviews Drug Discovery, 2014. **13**(3): p. 197-216.
35. Kallen, J.A., *et al*., *X-Ray Structure of the hRORalpha LBD at 1.63 A: Structural and Functional Data that Cholesterol or a Cholesterol Derivative Is the Natural Ligand of RORalpha.* Structure, 2002. **10**(12): p. 1697-1707.
36. Stehlin, C., *et al*., *X-ray structure of the orphan nuclear receptor RORβ ligand-binding domain in the active conformation.* The EMBO Journal, 2001. **20**(21): p. 5822-5831.
37. Jin, L., *et al*., *Structural Basis for Hydroxycholesterols as Natural Ligands of Orphan Nuclear Receptor RORγ.* Molecular Endocrinology, 2010. **24**(5): p. 923-929.
38. Soroosh, P., *et al*., *Oxysterols are agonist ligands of RORγt and drive Th17 cell differentiation.* Proc Natl Acad Sci U S A, 2014. **111**(33): p. 12163-8.
39. Hu, X., *et al*., *Sterol metabolism controls TH17 differentiation by generating endogenous RORγ agonists.* Nature Chemical Biology, 2015. **11**(2): p. 141-147.
40. Santori, Fabio R., *et al*., *Identification of Natural RORγ Ligands that Regulate the Development of Lymphoid Cells.* Cell Metabolism, 2015. **21**(2): p. 286-298.
41. Wang, Y., *et al*., *A second class of nuclear receptors for oxysterols: Regulation of RORα and RORγ activity by 24S-hydroxycholesterol (cerebrosterol).* Biochimica et Biophysica Acta (BBA) - Molecular and Cell Biology of Lipids, 2010. **1801**(8): p. 917-923.
42. Wang, Y., *et al*., *Modulation of Retinoic Acid Receptor-related Orphan Receptor alpha and gamma Activity by 7-Oxygenated Sterol Ligands.* Journal of Biological Chemistry, 2010. **285**(7): p. 5013-5025.
43. Kono, M., *et al*., *Discovery of [cis-3-({(5R)-5-[(7-Fluoro-1,1-dimethyl-2,3-dihydro-1H-inden-5-yl)carbamoyl]-2-methoxy-7,8-dihydro-1,6-naphthyridin-6(5H)-yl}carbonyl)cyclobutyl]acetic Acid (TAK-828F) as a Potent, Selective, and Orally Available Novel Retinoic Acid Receptor-Related Orphan Receptor γt Inverse Agonist.* Journal of Medicinal Chemistry, 2018. **61**(7): p. 2973-2988.
44. Shibata, A., *et al*., *Pharmacological inhibitory profile of TAK-828F, a potent and selective orally available RORγt inverse agonist.* Biochemical Pharmacology, 2018. **150**: p. 35-45.
45. Igaki, K., *et al*., *Pharmacological Evaluation of TAK-828F, a Novel Orally Available RORγt Inverse Agonist, on Murine Colitis Model.* Inflammation, 2019. **42**(1): p. 91-102.

46. Ichiyama, K., *et al*., *Foxp3 Inhibits RORgammat-mediated IL-17A mRNA Transcription through Direct Interaction with RORgammat.* Journal of Biological Chemistry, 2008. **283**(25): p. 17003-17008.
47. Thales, K., *et al*., *Nuclear Receptor Modulators — Current Approaches and Future Perspectives*, in *Drug Discovery and Development*, V. Omboon and O. Suleiman, Editors. 2015, IntechOpen: Rijeka. p. Ch. 5.
48. Fauber, B.P., *et al*., *Structure-based design of substituted hexafluoroisopropanol-arylsulfonamides as modulators of RORc.* Bioorganic & Medicinal Chemistry Letters, 2013. **23**(24): p. 6604-6609.
49. Pantoliano, M.W., *et al*., *High-density miniaturized thermal shift assays as a general strategy for drug discovery.* J Biomol Screen, 2001. **6**(6): p. 429-40.
50. Shirai, J., *et al*., *Discovery of orally efficacious RORγt inverse agonists, part 1: Identification of novel phenylglycinamides as lead scaffolds.* Bioorg Med Chem, 2018. **26**(2): p. 483-500.
51. Bitsch, F., *et al*., *Identification of natural ligands of retinoic acid receptor-related orphan receptor alpha ligand-binding domain expressed in Sf9 cells--a mass spectrometry approach.* Anal Biochem, 2003. **323**(1): p. 139-49.
52. Tripathi, N.K. and A. Shrivastava, *Recent Developments in Bioprocessing of Recombinant Proteins: Expression Hosts and Process Development.* Frontiers in Bioengineering and Biotechnology, 2019. **7**.
53. Vasseur, L., *et al*., *Importance of the Choice of a Recombinant System to Produce Large Amounts of Functional Membrane Protein hERG.* Int J Mol Sci, 2019. **20**(13).
54. Liu, F., *et al*., *Use of baculovirus expression system for generation of virus-like particles: successes and challenges.* Protein Expr Purif, 2013. **90**(2): p. 104-16.
55. Zhang, Y., *et al*., *ROR nuclear receptors: structures, related diseases, and drug discovery.* Acta Pharmacol Sin, 2015. **36**(1): p. 71-87.
56. Dhe-Paganon, S., *et al*., *Crystal structure of the HNF4 alpha ligand binding domain in complex with endogenous fatty acid ligand.* J Biol Chem, 2002. **277**(41): p. 37973-6.
57. Wisely, G.B., *et al*., *Hepatocyte nuclear factor 4 is a transcription factor that constitutively binds fatty acids.* Structure, 2002. **10**(9): p. 1225-34.
58. Briscoe, C.P., *et al*., *The orphan G protein-coupled receptor GPR40 is activated by medium and long chain fatty acids.* J Biol Chem, 2003. **278**(13): p. 11303-11.
59. Itoh, Y., *et al*., *Free fatty acids regulate insulin secretion from pancreatic beta cells through GPR40.* Nature, 2003. **422**(6928): p. 173-6.
60. Mancini, A.D. and V. Poitout, *The fatty acid receptor FFA1/GPR40 a decade later: how much do we know?* Trends Endocrinol Metab, 2013. **24**(8): p. 398-407.

61. Pais, R., F.M. Gribble, and F. Reimann, *Stimulation of incretin secreting cells.* Therapeutic advances in endocrinology and metabolism, 2016. **7**(1): p. 24-42.
62. Tsujihata, Y., *et al*., *TAK-875, an Orally Available G Protein-Coupled Receptor 40/Free Fatty Acid Receptor 1 Agonist, Enhances Glucose-Dependent Insulin Secretion and Improves Both Postprandial and Fasting Hyperglycemia in Type 2 Diabetic Rats.* Journal of Pharmacology and Experimental Therapeutics, 2011. **339**(1): p. 228-237.
63. Burant, C.F., *et al*., *TAK-875 versus placebo or glimepiride in type 2 diabetes mellitus: a phase 2, randomised, double-blind, placebo-controlled trial.* Lancet, 2012. **379**(9824): p. 1403-11.
64. Kaku, K., *et al*., *Long-term safety and efficacy of fasiglifam (TAK-875), a G-protein-coupled receptor 40 agonist, as monotherapy and combination therapy in Japanese patients with type 2 diabetes: a 52-week open-label phase III study.* Diabetes Obes Metab, 2016. **18**(9): p. 925-9.
65. Lin, D.C., *et al*., *Identification and pharmacological characterization of multiple allosteric binding sites on the free fatty acid 1 receptor.* Mol Pharmacol, 2012. **82**(5): p. 843-59.
66. Li, Z., *et al*., *Free fatty acid receptor agonists for the treatment of type 2 diabetes: drugs in preclinical to phase II clinical development.* Expert opinion on investigational drugs, 2016. **25**(8): p. 871-890.
67. Li, Z., Z. Zhou, and L. Zhang, *Current status of GPR40/FFAR1 modulators in medicinal chemistry (2016–2019): a patent review.* Expert Opinion on Therapeutic Patents, 2020. **30**(1): p. 27-38.
68. Lu, J., *et al*., *Structural basis for the cooperative allosteric activation of the free fatty acid receptor GPR40.* Nat Struct Mol Biol, 2017. **24**(7): p. 570-577.
69. Ho, J.D., *et al*., *Structural basis for GPR40 allosteric agonism and incretin stimulation.* Nat Commun, 2018. **9**(1): p. 1645.
70. Hauge, M., *et al*., *GPR40 (FFAR1) - Combined Gs and Gq signaling in vitro is associated with robust incretin secretagogue action ex vivo and in vivo.* Mol Metab, 2015. **4**(1): p. 3-14.
71. Rives, M.L., *et al*., *GPR40-Mediated Galpha12 Activation by Allosteric Full Agonists Highly Efficacious at Potentiating Glucose-Stimulated Insulin Secretion in Human Islets.* Mol Pharmacol, 2018. **93**(6): p. 581-591.
72. Defossa, E. and M. Wagner, *Recent developments in the discovery of FFA1 receptor agonists as novel oral treatment for type 2 diabetes mellitus.* Bioorg Med Chem Lett, 2014. **24**(14): p. 2991-3000.
73. Li, Z., *et al*., *Free Fatty Acid Receptor 1 (FFAR1) as an Emerging Therapeutic Target for*

Type 2 Diabetes Mellitus: Recent Progress and Prevailing Challenges. Med Res Rev, 2018. **38**(2): p. 381-425.

74. Kahn, S.E., *et al*., *Glycemic durability of rosiglitazone, metformin, or glyburide monotherapy.* N Engl J Med, 2006. **355**(23): p. 2427-43.
75. Drake, M.T., S.K. Shenoy, and R.J. Lefkowitz, *Trafficking of G protein-coupled receptors.* Circ Res, 2006. **99**(6): p. 570-82.
76. Kelly, E., C.P. Bailey, and G. Henderson, *Agonist-selective mechanisms of GPCR desensitization.* Br J Pharmacol, 2008. **153 Suppl 1**: p. S379-88.
77. Callander, G.E., W.G. Thomas, and R.A. Bathgate, *Prolonged RXFP1 and RXFP2 signaling can be explained by poor internalization and a lack of beta-arrestin recruitment.* Am J Physiol Cell Physiol, 2009. **296**(5): p. C1058-66.
78. Tirupula, K.C., *et al*., *Atypical signaling and functional desensitization response of MAS receptor to peptide ligands.* PLoS One, 2014. **9**(7): p. e103520.
79. Chen, Y., *et al*., *A selective GPR40 (FFAR1) agonist LY2881835 provides immediate and durable glucose control in rodent models of type 2 diabetes.* Pharmacol Res Perspect, 2016. **4**(6): p. e00278.
80. Chen, Y., *et al*., *HWL-088, a new potent free fatty acid receptor 1 (FFAR1) agonist, improves glucolipid metabolism and acts additively with metformin in ob/ob diabetic mice.* Br J Pharmacol, 2020.
81. Yabuki, C., *et al*., *A novel antidiabetic drug, fasiglifam/TAK-875, acts as an ago-allosteric modulator of FFAR1.* PLoS One, 2013. **8**(10): p. e76280.
82. Portha B, M.J., Cuzin-Tourrel C, Bailbe D, Giroix M, Serradas P, Dolz M and Kergoat M, *Neonatally streptozotocin-induced (n-STZ) diabetic rats: a family of type 2 diabetes models.* Animal Models of Diabetes, 2007.
83. Levetan, C., *Oral antidiabetic agents in type 2 diabetes.* Current Medical Research and Opinion, 2007. **23**: p. 945 - 952.
84. Brown, S.P., *et al*., *Discovery of AM-1638: A Potent and Orally Bioavailable GPR40/FFA1 Full Agonist.* ACS Med Chem Lett, 2012. **3**(9): p. 726-30.
85. Ueno, H., *et al*., *SCO-267, a GPR40 Full Agonist, Improves Glycemic and Body Weight Control in Rat Models of Diabetes and Obesity.* J Pharmacol Exp Ther, 2019. **370**(2): p. 172-181.
86. Srivastava, A., *et al*., *High-resolution structure of the human GPR40 receptor bound to allosteric agonist TAK-875.* Nature, 2014. **513**(7516): p. 124-7.
87. Buse, J.B., *et al*., *Effects of exenatide (exendin-4) on glycemic control over 30 weeks in sulfonylurea-treated patients with type 2 diabetes.* Diabetes Care, 2004. **27**(11): p. 2628-35.

88. Drucker, D.J., *et al*., *Exenatide once weekly versus twice daily for the treatment of type 2 diabetes: a randomised, open-label, non-inferiority study.* Lancet, 2008. **372**(9645): p. 1240-50.
89. Ito, R., *et al*., *TAK-875, a GPR40/FFAR1 agonist, in combination with metformin prevents progression of diabetes and β-cell dysfunction in Zucker diabetic fatty rats.* British journal of pharmacology, 2013. **170**(3): p. 568-580.
90. Sandoval, D.A. and D.A. D'Alessio, *Physiology of proglucagon peptides: role of glucagon and GLP-1 in health and disease.* Physiol Rev, 2015. **95**(2): p. 513-48.
91. Bonner-Weir, S., *et al*., *Responses of Neonatal Rat Islets to Streptozotocin: Limited B-Cell Regeneration and Hyperglycemia.* Diabetes, 1981. **30**(1): p. 64-69.
92. Kaiser, N., G. Leibowitz, and R. Nesher, *Glucotoxicity and beta-cell failure in type 2 diabetes mellitus.* J Pediatr Endocrinol Metab, 2003. **16**(1): p. 5-22.
93. Du, T., *et al*., *Vincamine as a GPR40 agonist improves glucose homeostasis in type 2 diabetic mice.* Journal of Endocrinology, 2019. **240**(2): p. 195-214.
94. Verma, M.K., *et al*., *Activation of GPR40 attenuates chronic inflammation induced impact on pancreatic β-cells health and function.* BMC Cell Biology, 2014. **15**(1): p. 24.
95. Wootten, D., *et al*., *Allosteric modulation of endogenous metabolites as an avenue for drug discovery.* Mol Pharmacol, 2012. **82**(2): p. 281-90.
96. Nakamura, Y., *et al*., *Pharmacological evaluation of TAK-828F, a novel orally available RORγt inverse agonist, on murine chronic experimental autoimmune encephalomyelitis model.* Journal of Neuroimmunology, 2019. **335**: p. 577016.
97. Scheepstra, M., *et al*., *Identification of an allosteric binding site for RORγt inhibition.* Nature Communications, 2015. **6**(1): p. 8833.
98. Saenz, S.A., *et al*., *Small molecule allosteric inhibitors of RORγt block Th17-dependent inflammation and associated gene expression in vivo.* PLoS One, 2021. **16**(11): p. e0248034.
99. Rutz, S., *et al*., *Post-translational regulation of RORγt-A therapeutic target for the modulation of interleukin-17-mediated responses in autoimmune diseases.* Cytokine Growth Factor Rev, 2016. **30**: p. 1-17.
100. Furuyama, K., *et al*., *RORγt+Foxp3+ regulatory T cells in the regulation of autoimmune arthritis.* Clin Exp Immunol, 2022. **207**(2): p. 176-187.
101. Zou, H., *et al*., *Nuclear receptor RORγ inverse agonists/antagonists display tissue- and gene-context selectivity through distinct activities in altering chromatin accessibility and master regulator SREBP2 occupancy.* Pharmacological Research, 2022. **182**: p. 106324.
102. Gege, C., *Retinoic acid-related orphan receptor gamma t (RORγt) inverse agonists/antagonists for the treatment of inflammatory diseases – where are we*

presently? Expert Opinion on Drug Discovery, 2021. **16**(12): p. 1517-1535.

103. Sun, Z., *et al*., *Requirement for RORgamma in thymocyte survival and lymphoid organ development.* Science, 2000. **288**(5475): p. 2369-73.
104. Haggerty, H.G., *et al*., *Thymic Lymphomas in a 6-Month rasH2-Tg Mouse Carcinogenicity Study With the RORγt Inverse Agonist, BMS-986251.* Toxicol Sci, 2021. **183**(1): p. 93-104.
105. Arab, J.P., M. Arrese, and M. Trauner, *Recent Insights into the Pathogenesis of Nonalcoholic Fatty Liver Disease.* Annu Rev Pathol, 2018. **13**: p. 321-350.
106. Ookawara, M., *et al*., *The GPR40 full agonist SCO-267 improves liver parameters in a mouse model of nonalcoholic fatty liver disease without affecting glucose or body weight.* Journal of Pharmacology and Experimental Therapeutics, 2020. 375(1):p. 21-27.
107. Nishizaki, H., *et al*., *SCO-267, a GPR40 Full Agonist, Stimulates Islet and Gut Hormone Secretion and Improves Glycemic Control in Humans.* Diabetes, 2021. **70**(10): p. 2364-2376.
108. Krupnick, J.G. and J.L. Benovic, *The role of receptor kinases and arrestins in G protein-coupled receptor regulation.* Annu Rev Pharmacol Toxicol, 1998. **38**: p. 289-319.
109. Lefkowitz, R.J., *A Brief History of G-Protein Coupled Receptors (Nobel Lecture).* Angewandte Chemie International Edition, 2013. **52**(25): p. 6366-6378.
110. Tobin, A.B., *G-protein-coupled receptor phosphorylation: where, when and by whom.* British Journal of Pharmacology, 2008. **153**(S1): p. S167-S176.
111. Prihandoko, R., *et al*., *Distinct Phosphorylation Clusters Determine the Signaling Outcome of Free Fatty Acid Receptor 4/G Protein–Coupled Receptor 120.* Molecular Pharmacology, 2016. **89**(5): p. 505-520.
112. Rajagopal, S., K. Rajagopal, and R.J. Lefkowitz, *Teaching old receptors new tricks: biasing seven-transmembrane receptors.* Nat Rev Drug Discov, 2010. **9**(5): p. 373-86.
113. Kohout, T.A., *et al*., *Differential desensitization, receptor phosphorylation, beta-arrestin recruitment, and ERK1/2 activation by the two endogenous ligands for the CC chemokine receptor 7.* J Biol Chem, 2004. **279**(22): p. 23214-22.
114. Wang, G., Z. Wei, and G. Wu, *Role of Rab GTPases in the export trafficking of G protein-coupled receptors.* Small GTPases, 2018. **9**(1-2): p. 130-135.
115. Schwartz, S.L., *et al*., *Rab GTPases at a glance.* Journal of Cell Science, 2007. **120**(22): p. 3905-3910.
116. Irannejad, R., *et al*., *Conformational biosensors reveal GPCR signalling from endosomes.* Nature, 2013. **495**(7442): p. 534-538.
117. Flores-Espinoza, E., *et al*., *Effect of docosahexaenoic acid, phorbol myristate acetate, and insulin on the interaction of the FFA4 (short isoform) receptor with Rab proteins.*

European Journal of Pharmacology, 2020. **889**: p. 173595.

118. Qian, J., *et al*., *Differential requirements of arrestin-3 and clathrin for ligand-dependent and -independent internalization of human G protein-coupled receptor 40.* Cell Signal, 2014. **26**(11): p. 2412-23.